MEASUREMENTS IN LIQUID FUEL SPRAYS

NASA Cooperative Agreement NCC 3-37

FINAL REPORT

12/15/83 - 12/14/85

Norman Chigier
Chien-Pei Mao

Department of Mechanical Engineering
Carnegie-Mellon University
Pittsburgh, PA 15213

1. INTRODUCTION

To successfully achieve all weather operation of military aircraft and rotorcraft, a thorough understanding of the adverse weather effects on the aircraft performance is required. It is for this reason that research on the effects of icing, snow and heavy rain has been carried out at NASA for several years. So far, most of the tests have been performed using expensive, time consuming and dangerous flight testing. A unique ground test facility is being established at NASA Lewis Research Center to simulate the environmental and flight conditions needed to study adverse weather effects. One of the most important components in this ground test facility is the water spray system which consists of many nozzles fitted on spray bars. Water is injected through air-assisted atomizers to generate uniform size drops to simulate natural icing in clouds.

The air-assist atomizer uses pressurized air to enhance the atomization produced by pressurized liquid. The atomization of liquid is primarily achieved by the shear forces due to high speed air flows. The major requirement is to generate uniform size water drops with control at the test section of the wind tunnel so that realistic environments can be achieved. Typical water drop sizes in icing clouds range from 5 to 60 μm, mass median diameter. The performance and characteristics of the air-assisted atomizer designed by NASA Lewis are being studied at CMU in order to determine the requirements for simulating icing clouds. Therefore, the primary objective of the present investigation is to provide experimental data on drop size distribution over a wide range of operating conditions. Correlation equations for mean drop size and initial injection parameters are being determined to assist in the design and modification of the Altitude Wind Tunnel. Special emphasis is being placed on the study of the aerodynamic structure of the air-assisted atomizer sprays. Detailed measurements of the variation of drop size distribution and velocity as a function of time and space are being made. A second objective is to provide accurate initial and boundary conditions for computer model evaluation.

A number of instruments including high magnification photography, laser diffraction, and the phase doppler analyzer are being used to make the measurements of spray angle, line-of-sight drop size distribution, and local point information such as drop size, velocity, liquid flux, and number density. The current drop velocity measurements using the phase doppler analyzer are limited to low liquid injection conditions due to the restricted instrument response. The higher frequency signal measurements will be pursued by adding optical frequency shifting such that the

Doppler frequency of the scattered light signal is optically downshifted into the operating range of the processor.

A comparative study of the data being obtained by photography, laser diffraction, and phase doppler on mean drop size distribution has shown inconsistent results at the same operating flow conditions. The differences in SMD are related to the limitations in dynamic range, detector response, sampling techniques, and sampling time of each instrument. An "ultimate" SMD could be measured provided that these limitations are suppressed and all drops are measured over a "long enough" time to cover all the possible low and high frequencies in the systems. None of the instruments are currently capable of measuring this "ultimate" SMD. Therefore, comparative measurements using different instruments are always subject to a certain degree of disagreement. Photography has the problems of obtaining statistically representative results and of not counting extremely large numbers of unfocused small drops. The laser diffraction particle sizer is limited by the threshold sensitivity of the diodes and the small detecting area of the inner diode rings. The relatively small number of large drops are overshadowed by a huge amount of small drops which reduce the sensitivity of the inner diodes which have relatively small area. In principle, the phase doppler particle analyzer has the potential of detecting the "ultimate" SMD of the sprays. It also provides the capability of examining particular sections of the size distribution spectrum that are of particular interest, by varying the threshold level of the processor and the high voltage of the detector. However, this capability is restricted by the instrument dynamic range and detector response.

2. EXPERIMENTS

The aim of the present investigation is to find correlation equations for predicting SMD (Sauter Mean Diameter) over a wide range of injection conditions to assist icing tunnel design and to establish a data base for computer model evaluation. The water mass flow rates that are being studied range from 10 lbm/hr to 100 lbm/hr. This corresponds to injection pressures ranging from 10 psi to 205 psi. The mass flow rate of air ranges from 20 lbm/hr to 150 lbm/hr which corresponds to a pressure injection range from 10 to 155 psi. Experiments are carried out in two different sizes of spray chambers under well-controlled flow conditions to accommodate both high and low water/air mass flow rate ratios.

Spray Chambers

Two spray chambers are being used for testing. Fig. 1 shows the configuration of the small scale spray chamber. This chamber was designed to accommodate maximum water flow rates of 40 lbm/hr. The cross-sectional area of the chamber is 12x12 inches and the window viewing area is 12x14 inches. A traversing system installed in the chamber provides 2-D freedom of motion of the atomizer without requiring the diagnostic instruments to be moved. For injection conditions of water/air mass flow rate ratio less than 1, strong recirculating flows are created in the chamber which significantly perturb the sprays. The large scale spray chamber is, therefore, used for examining the high speed liquid flows. Fig. 2 shows a schematic of the large scale spray chamber. This system is capable of providing maximum flow rates of 1200 lbm/hr for water and 190 lbm/hr for air. The four-sided, glass walled spray chamber has a cross sectional area of 20x25 inches. The window height is 29 inches. A secondary air flow, produced by the suction of a high power blower, eliminates the flow recirculation and fogging of the window. The advantages of the large scale chamber are: wider range of test conditions, no recirculation, measurements can be made farther downstream (up to 30 inches downstream from the atomizer orifice), and a larger working distance. The disadvantage is that the larger cross sectional distance is approaching the critical value of vignetting so that receiving lenses less than 300 mm cannot be used for data acquisition. The small spray chamber, on the contrary, is much easier to operate and allows more accurate control of the flow rates.

Atomizers

Two atomizers have been received from NASA for testing. They are numbered as nozzle 100 and 2, respectively. These two atomizers have the same nozzle design (see Fig. 3), but with different flow rates at the same injection conditions. A careful calibration of the water volume flow rates of these two atomizers was made. Fig. 4 shows the water volume flow rates versus differential pressures for both the number 100 and 2 atomizers. The "differential pressure" refers to the pressure difference between water injection and air injection at the atomizer exit in units of psi. Both the number 100 and number 2 atomizers have been tested in the present investigation. Qualitatively, these two atomizers have similar characteristics. As indicated in Fig. 4, #100 nozzle has a higher volume flow rate than that of #2 nozzle at the same differential pressures. For nozzle #100, all data of volume flow rates fit well with the following equation,

$$\dot{v} = 0.81 \ \sqrt{\Delta P}$$

where $\dot{v}$ is the water volume flow rate in gallons per hour, and δP is the differential pressure in psi. As for nozzle #2, it was also found that water volume flow rate is proportional to the square root of differential pressure,

$$\dot{v} = 0.609 \ \sqrt{\Delta P}$$

Although these two nozzles have the same design, the water mass flow rates are different. The differences are found due to the surface roughness at the nozzle exit. Nozzle #100 has much rougher lips at the exit. The nominal diameter of the orifice is essentially bigger for nozzle 100. In the #100 air-assisted atomizer, the pressure of air flow affects the pressure of liquid injection. Fig. 5 shows the mass flow rate of air versus gauge pressure with and without water injection for nozzle #100. The mass flow rates of air are linearly proportional to the gauge pressure in the nozzle. Under the water injection condition, the mass flow rates of air are slightly decreased due to the decrease of the cross-sectional area at the nozzle exit. Fig. 6 shows the air mass flow rates versus the gauge pressure for nozzle #2.

Photography

Still photography is used as the standard means for visualization and preassessment of global spray structure. It also provides a calibration intermediate between the standard calibrating devices (reticule and impulsed drop generator) and other instruments with high data acquisition rate. A low magnification 35 mm Canon F-1 camera with near forward lighting technique is used to determine the spray angle. The light source is a Koolbeam light bulb array which consists of 300 W tungsten halogen lamps. Measurements of the spray angle are made by setting the camera at f/11 and 1/125 second time exposure. These settings are selected to provide high contrast and consistent spray angles since spray angle can be changed by varying the light exposure. A high magnification 4x5 inches format camera with a 5 feet and a 10 feet long bellows is also used to examine local spray structure. The high speed, high intensity EG&G 549 microflash light source is utilized to freeze the high speed drop motion and to provide enough light scattering intensity from the smaller drops.

Laser Diffraction Particle Sizer

For a rapid analysis of the spray characteristics, the laser diffraction particle sizer is currently the most effective instrument at CMU. Line-of-sight mean drop size, size distribution and liquid volume concentration information are provided by this instrument. The instrument is based on the detection of near-forward Fraunhofer diffraction. It is rather simple in operation and is efficient in data acquisition.

However, there are many limitations associated with the detection technique. Extensive studies of the accuracy and limitations of the laser diffraction particle sizer have been made at CMU. The major problem with this instrument is obtaining accurate drop size spectra in sprays due to the lack of the capability of "seeing" the small fraction of large drops which are clearly seen in photographic pictures. Results have shown that this problem is more severe at extremely high and low obscuration conditions. Nevertheless, the laser diffraction particle sizer is used as the principal instrument for determining representative drop sizes in sprays. Measurements are made at several selected downstream axial and radial stations. At each axial location, the atomizer is traversed radially across the laser beam to obtain radial size distributions. A horizontal plane averaged SMD is obtained by taking into account the non-uniform liquid volume concentration distribution for drop size correlation.

Phase Doppler Spray Analyzer

This instrument is used for detailed local drop size and velocity measurements in the sprays. It was developed by Bachalo and Houser[1]. The technique is based upon the measurement of the interference fringe pattern produced by spherical drops passing through the intersection of two laser beams. Three detectors, separated at fixed spacing, are used to receive doppler signals and to determine the phase shift due to different path lengths of the laser beam. The spatial frequency of the interference fringe pattern is linearly proportional to the measured drop size. The most important capability of this instrument is that it provides simultaneous drop size and velocity measurements. Other local point information provided by this instrument include: liquid flux, number density, size-velocity correlation, spatial and temporal mean drop sizes. A detailed validation study has been performed to determine the limitations and accuracy of this instrument. A rotating disk and an impulsed piezoelectric drop generator are used as calibration devices. A number of problems with this instrument have been found during the validation study. They include: an inconsistency in measured velocities which differed at times by a factor of 2, a complete lock-up at certain filter selections, and general failure of certain configurations to provide reliable data. These problems have been corrected by the manufacturer and they were recognized to be caused by a digital board trace short, incomplete trace cuts on the processor motherboard, and improper plastic connector shells on cables. From our experience, all optical configurations (which determine different measurement ranges) require to be examined before use. Otherwise, any of the problems mentioned above may arise with certain optical configurations and may not be easily detected. Our instrument has an upper doppler frequency limit of 3.2 MHz due to the limitation of the detector/preamplifier response. It is for this reason

that the phase doppler spray analyzer is currently being used only for measuring very low water injection conditions which have lower drop velocities. The system will be upgraded by purchasing a rotating grating frequency shifter to enable higher speed flows to be measured so that the whole range of injection conditions can be examined.

3. RESULTS AND DISCUSSION

Breakup Mechanism and Atomization

Fig. 7 to Fig. 14 are shown to demonstrate the typical air-assist spray structure and the process of atomization. Air-assist atomizers employ the kinetic energy of air flow to tear the water jet into ligaments and subsequently into various sizes of drops. Fig. 7 shows that water emerges from the orifice as a circular jet with very high speed. The water circular jet is very unstable, even under the condition of no air injection. The oscillation of the jet causes the formation of necking and the amplitude of the oscillation grows with downstream distance. Any distortion of the water jet surface due to oscillation is opposed by surface tension forces. Through several stages of force balance, ligaments and satellite drops are formed between the necks. The atomization can be highly improved by injecting the water into a high-velocity airstream. Fig. 8 to Fig. 14 show the effect of increasing air velocity on atomization. Apparently, Fig. 14 shows the best atomization due to higher air velocity. In fact, the NASA air-assist atomizer is very similar to the Nukiyama-Tanasawa[2] atomizer. At a fixed water injection pressure, the mean drop size decreases with the increase of air flow rates or decreases with the increase of relative velocity. In the flow field near to the atomizer, the velocity of air is much higher than that of the water. The velocity of air was estimated to be close to sonic velocity at all test conditions. The inverted "V" shape of the spray near the orifice indicates that the water jet is surrounded by high speed air flow and is dragged by the air in the direction of the air flow. The velocity of air relaxes much faster than the liquid flow velocity as downstream distance increases. The global shape of the spray is seen to be converted into a "V" shape far downstream where the velocity of liquid is faster than the velocity of air. It is also noted that the angle of the inverted "V" shape in the near flow field increases with the increase of air mass flow rates. Thus, the increase of air velocity increases the surface of interaction between the liquid and air which enhances the atomization. In the very inner section of the water jet, a group of ligaments and large drops retain their initial high velocity without too much interaction with the surrounding air. The penetration distance of ligaments and large drops, in the cases of fixed liquid

injection pressure, depends on the initial air mass flow rates. Since the relative velocity between water and air is kept the same for Figs. 8 to 14, the mass flow rate of air is the only dominant factor that influences the quality of atomization. More than 200 photographic observations show that the NASA air-assist atomizer spray structure is very similar to that of diesel jet sprays which are being studied separately at Carnegie Mellon University. The breakup processes occur periodically and consist of a series of inverted "V" shape sprays. The liquid water is mostly concentrated in the center of each inverted "V" group and becomes more dilute as the "V" shape spreads out radially. Scattered satellite drops were found between each inverted "V" group. This observation shows that the spray breakup is not a continuous process but very oscillating. Measurements should be made with "long enough" time so that a statistically representative result can be assured.

Figs. 15 to 20 show the close-up look of NASA air-assist atomizer sprays at several centerline downstream locations at the condition of water injection 58.7 psi and air injection 10 psi. The use of the 4x5 inch format camera with a 10 ft. bellows allows us to visualize an area of 9x9 mm^2 inside the sprays. These pictures show much more detail about the breakup process and drop size distribution. Fig. 15 shows that the initial atomization starts at the periphery of the water jet. The shear forces tear and shatter the water jet surface apart. The center core is so dense that almost no light can penetrate. Fig. 17 shows that long ligaments are formed at x=4.5 cm downstream. The surface tension is struggling to rearrange the shape of the ligaments. However, adverse pressure of air tends to further break down. The process of atomization is actually slowed down with downstream distance because of the quick deceleration of the air flows. The redistribution of drop size and drop velocity at downstream stations causes collision between drops. In Fig. 21, a few large drops are about to separate from the small drops after collision. The bridge between them is the source of satellite drops after the breakup. The phenomenon of drop collision has been studied by several researchers[3,4] in the past. The effect of collision on drop size distribution can be categorized into two groups: (1) drops coalesce after collision , and (2) satellite drops are created after collision. The former effect leads to an increase in the mean drop size and the latter effect leads to a decrease in the mean drop size. The efficiency of collision depends on the Weber number at the moment of collision. A two color phase doppler system designed for measuring two components of drop velocity can be used to evaluate the efficiency of collision at a local point by calculating the Weber number of size bins. By observing these magnified pictures, a small number of large drops in the

size range from 300 μm to 500 μm diameter can be easily seen even at downstream distance 13.5 cm where atomization is already completed. Comparisons between photographs and data obtained from the laser diffraction particle sizer have shown inconsistencies in drop size distribution, especially regarding the large drops in the sprays. Further analysis of the photographic results using an automated digital imaging system[5] is necessary to provide long time statistical averaging drop size information.

The spray cone angle is also measured using a near forward lighting technique. All pictures were taken under the same optical setting and with the same films. The camera was set at the f/11 aperture with a 1/125 second time exposure. A Kodak Tri-X film was used to obtain high contrast pictures. The spray angle was measured over a wide range of operating conditions. The water injection pressure was tested from 35 psi to 325 psi and the air injection pressure was varied from 25 psi to 155 psi. There was no special trend found for the spray angle with respect to the pressure variation. It actually oscillates with pressure. In general, the global spray angle varies between 19° and 25°. The fine drops that surround the main water jet affect the accurate determination of the spray boundary due to longer exposure time. However, the angle of the inverted "V" shape in the flow field near the atomizer varies with the mass flow rates of air (see Fig. 8 to 14). The higher the mass flow rate of air, the wider the angle of the inverted "V" shape. Fig. 23 gives an example of the picture obtained using the near forward lighting technique for the determination of spray cone angle.

Downstream Drop Size Variation

Line-of-sight mean drop size measurements were first made using nozzle #100 at various downstream locations over a wide range of injection conditions. Since the distance for complete breakup was quite long, the 4x5 format camera was used to examine the first downstream measurement station. Fig. 24 shows the radial SMD distribution at several downstream stations at P_w= 35 psi and P_{air}= 25 psi for nozzle #100. The size distribution is found to be quite uniform across the sprays at all locations. But, the mean drop sizes increase with the increase of downstream distance. Fig. 25 shows the radial SMD distribution at several downstream stations for P_w= 65 psi and P_{air}= 25 psi. By comparing Fig. 25 with Fig. 24, the radial size distribution is no longer uniform across the spray due to the increase of water injection pressure. The maximum SMD peaks at a position slightly off the center axis. A common feature for both cases is that the SMD increases gradually with the downstream distance. Further increase of the water injection pressure increases the

non-uniformity of the radial size distribution. The symmetry of the size distribution is also greatly distorted at higher water injection conditions. Fig. 26 indicates the shifting of the peak SMD position as a function of distance at P_w= 200 psi and P_{air}= 25 psi. As can be seen, the mean drop size varies considerably across the sprays. There is no single SMD that can be used to represent the entire spray. A judicious decision has to be made for selecting appropriate values of SMD to fit existing empirical correlation equations. Further details of drop size correlation will be given in the next section.

In order to simulate the icing clouds in the wind tunnel, it is required that a uniform drop size distribution be produced by the nozzle. Based on the measurements made at many axial and radial stations over a wide range of injection conditions on nozzle #100, it was found that the structure of NASA air-assist atomizer sprays can be separated into two categories depending on the water/air mass flow rate ratios. For a water/air mass flow rate ratio of less than 1, no matter how high the injection pressures were, the radial mean drop size distribution is rather uniform as seen in Fig. 24 and gradually increases with axial downstream distance. For water/air mass flow rate ratio greater than 1, the radial mean drop size distribution is nonuniform. It peaks at a position somewhere off the center axis. The deviation of the peak SMD position from the center line increases with the downstream distance. The characteristic of the NASA air-assist atomizer sprays of not being symmetric as water/air mass flow rate ratios increases is not completely due to the aerodynamic instability effect. It is partially due to the original tilting of the water jet tube inside the nozzle. Nevertheless, the nonsymmetry of the spray is not going to affect the evaluation and correlation of size distribution based upon planar averaged drop size distribution at each axial station. Fig. 27 shows another example of a uniform radial SMD distribution at high water injection pressure conditions for nozzle #100. The water/air mass flow rate ratio is close to 1. Fig. 28 indicates that the mean drop size is increasing along the downstream distance and the size distribution is not very uniform across the sprays for water/air mass flow rate ratios much greater than 1. For the purpose of simulating icing clouds, it is therefore suggested that the operation of nozzle injection pressures be maintained at the conditions of water/air mass flow rate ratios less than 1 so that uniform drop size can be produced. Up to this point, all discussions have been based upon the results obtained for NASA nozzle #100. From this point on, all of the tests were conducted using NASA nozzle #2, and measurements were made for the injection conditions that provide a water/air mass flow rate ratio less than 1. Nozzle #2 was

manufactured to high precision, and it is identical to other nozzles (Ref. 6) also being tested by NASA Lewis Research Center.

In general, these two nozzles (100 and 2) showed similar characteristics in spray structures. The size distribution, however, differs in magnitude. Further details about the NASA air-assist atomizer sprays are discussed based on the measurements of nozzle #2. Fig. 29 shows a picture taken by the high magnification 4x5 inches format camera at 15 cm downstream from the atomizer with water injection pressure 59 psi and air injection pressure 10 psi. By comparing many photographs such as this and laser diffraction measurements at the same locations, it has become clear that there is a number of large drops in the sprays. This raises the question of whether the uniform drop size distribution measured by the laser diffraction particle sizer is accurate or not. These large drops that are seen in the photographs can play an important role in the simulation of icing clouds in the altitude wind tunnel. In addition, the reported phenomena of continuous increase in measured downstream drop size has to be carefully examined to establish whether water drops continue to increase in size until they reach the test section of the wind tunnel. Currently, the effects of drop acceleration/deceleration, collision/coalescence, and evaporation on downstream size variation are being studied in our laboratory. Evidence has been found that drops do have a strong tendency to coalesce after collision[3]. The deceleration of drops causes interaction and collision and results in a subsequent increase in drop size.

Another problem associated with the laser diffraction technique is the preselection of the size distribution mode. Throughout the present investigation, a Rosin-Rammler size distribution function was chosen $R = \exp[- (D/\bar{x})^N]$, where R is the volume fraction of particles with a diameter greater than D, N is the parameter related to the polydispersity of the distribution, and $\bar{x}$ is a representative mean diameter such that 36.8% of the total particle volume is greater than $\bar{x}$. However, it is found that this size distribution function may not be valid throughout the sprays. Fig. 30 shows an example of a good fit using the Rosin-Rammler (2 parameters) and model independent (15 parameters) modes to obtain the weight fraction distribution. In the region inside the spray, with higher obscuration, the Rosin-Rammler mode is acceptable for obtaining accurate size distribution. However, the Rosin-Rammler mode fails to predict the large size drops at the edge of the sprays where there is low obscuration. Fig. 31 shows that the model independent mode provides a more accurate determination of the large drops that are present near the edge of the

sprays. In general, the Rosin-Rammler mode can be applied to most areas of the NASA atomizer sprays except the region near the spray boundaries where the model independent mode has to be used in order to get more accurate SMDs. However, it was also noted that the Rosin-Rammler size distribution mode is not appropriate for drop size calculations even at the center positions under extremely high water/air mass flow rate ratios (>1).

Mean Drop Size Correlation

Empirical mean drop size correlation equations have been widely used for describing the characteristics and structure of various types of atomizer sprays. There is no universal equation that is suitable for all sprays. In the present study for NASA air-assist atomizer sprays, drop size correlations as a function of initial input parameters were determined based upon the line-of-sight laser diffraction particle sizer measurements for nozzle #2. Since the drop size varies all over the spray, it has been arbitrarily selected that all measurements be made at a fixed axial location 25 inches downstream from the atomizer where complete atomization is definitely achieved for all conditions. Fig. 32 shows the radial SMD distributions for several different water injection pressures. The air injection pressure was kept the same at 65 psi. All five test conditions were measured at the axial station 25 inches from the nozzle, and all water/air mass flow rates are less than 1. Although all test conditions have uniform drop size distribution, a planar averaged SMD is calculated from each local radial SMD across the spray by taking into account the radial liquid volume concentration distribution. A plane averaged SMD is more appropriate to represent the entire spray and to derive empirical correlation equations. Fig. 33 is a summary of the variation of SMD with respect to differential pressures (P_w-P_{air}) for the NASA #2 nozzle. At fixed air injection pressures, the SMD increases with the increase in water injection pressure. At fixed water injection pressure the SMD decreases with the increase of air pressures. There is a more significant increase in SMD by increasing water injection pressures at lower air pressures. At the high air injection pressures, the increase of water pressure or flow rates has no effect on mean drop size variation.

There are many published equations for the prediction of SMD of various types of atomizers. Several data fit equations are considered based upon the characteristics of the nozzle, physical process of atomization, and possible dominant parameters of the injection fluid flows.

(1) $\text{SMD} \sim \left(1 + \dfrac{\dot{m}_L}{\dot{m}_A} \right)^{0.5} / V_R$

(2) $\text{SMD} \sim \dot{m}_L / \dot{m}_A$

(3) $\text{SMD} \sim \left(\dot{m}_L / \dot{m}_A \right)^{1.5}$

where V_R is the initial relative velocity between the water and air. None of the above correlations fit the data as well as the Simmons SF7 equation[7]. Simmons derived an equation for air-assist simplex nozzles based upon the concept of hypothetical film thickness and relative interaction of liquid and air. We found that this equation also predicts very well the SMD for the NASA air-assist atomizer. Fig. 34 shows the results of the SMD correlation with respect to the grouping parameter,

$$\text{SMD} \sim \rho_A^{-0.325} \left(\frac{\dot{m}_L}{\dot{m}_L V_L + \dot{m}_A V_A} \right)^{0.55}$$

where ρ_A is the density of air at injection pressure, $\dot{M}_L$ is the mass flow rate of water, V_L is the exit velocity of liquid, $\dot{M}_A$ is the air mass flow rate, and V_A is the air exit velocity. This correlation equation can provide useful information about drop size distribution at different operating conditions to assist in wind tunnel design.

Local Drop Size and Velocity Measurements

The measurements of local drop size and velocity are extremely important for spray structure analysis and computer model evaluation. The newly developed light scattering technique, the phase doppler spray analyzer, is being used to provide information on local mean velocity, velocity fluctuations, SMD, liquid flux, and number density. Since the instrument has an upper doppler frequency limit of 3.2 MHz and a dynamic range of 30, several injection conditions within the measurable range were selected for tests in the small scale chamber. The maximum downstream distance that can be measured is 17 cm from the nozzle exit. Table 1 is a summary of the phase doppler spray analyzer results for water flow rate of 45.3 lbm/hr and air flow rate of 19.4 lbm/hr at axial station 17 cm. All current test conditions are limited to water/air mass flow ratios greater than 1 and they all show qualitatively similar spray structures. In general, the spray structure for water/air mass flow rate greater than 1 can be summarized as follows: the radial profile of mean axial drop

velocity sharply peaks at the center of the sprays. Most of the drops travelling in the center line region possess very high speed which is independent of drop size. There is no indication of mean drop velocity relaxation along the centerline within the 17 cm distance that has been measured. The measured velocity fluctuations (rms) have shown a gradual increase along the radial distance with a subsequent decrease towards the outer edge of the spray. Liquid volume flux (cc/sec) is also determined from the phase doppler spray analyzer measurement; these show almost the same radial profiles and magnitude at various axial locations. This indicates that spray evaporation is insignificant within the measured downstream distance. The liquid volume flux peaks at the centerline and then decreases sharply along the radial distance. The radial number density normally increases from the center axis and reaches a maximum at a point close to the edge of the spray. The higher number density region will result in higher possibilities of drop collision and coalescence. The increasing effect of drop collision toward the edge of the spray results in an increase of the drop size spectrum. Photographic evidence indicates that collisions are taking place. The radial drop size distribution indicates that the local SMD decreases along the radial distance from a peak at the centerline of the sprays. By comparing with the line-of-sight laser diffraction measurements, the local SMDs measured by the phase doppler analyzer are much larger. Since the laser diffraction particle sizer provides the particle size information in an in-line method with rather poor spatial resolution, there is a small quantity of large drops which are not "seen" by this instrument. The results reported by the laser diffraction technique can thus be in error. The inconsistency in the drop size distributions reported by these two techniques needs to be resolved by the imaging technique. The development of an automated digital imaging system is underway in our laboratories to assist the comparative study of spray structures using different instruments.

4. SUMMARY

In the present investigation, two well controlled spray facilities for testing NASA air-assist atomizers used in icing research have been constructed and calibrated. Interesting results about the spray aerodynamic structure have been observed. Under all test conditions, it was found that water/air mass flow rate ratio is a useful parameter to determine whether or not the drop sizes are uniform across the sprays. For water/air mass flow rate ratio greater than 1, the radial mean drop size is not uniform across the sprays. For water/air mass flow rate ratios less than 1, the radial mean drop size is uniformly distributed across the sprays. The gradual increase of SMD along downstream distance is a phenomenum associated with the aerodynamic effects and needs to be examined at distances farther downstream (>30

inches from atomizer). Drop deceleration and collision are the main factors causing SMD to increase along downstream distance. Simmons[7] drop size correlation equation was found to be suitable for predicting the SMD's for NASA air-assist atomizers over a wide range of injection conditions.

Comparisons between laser diffraction and photographic measurements are leading us to believe that the small area of the inner diodes, the threshold sensitivity of the diodes, and the relatively small number of large drops are resulting in insensitivity of the laser diffraction technique to the presence of the larger drops. For this reason, the laser diffraction instrument reports much smaller mean drop sizes at various locations than those measured by photography. However, it also needs to be pointed out that the photographic results are also neglecting a very large quantity of small drops. True "ultimate" SMD is unable to be measured by any of these two techniques.

A newly developed drop sizing instrument, phase doppler spray analyzer, was successfully applied to measure high speed flows in NASA atomizer sprays. Useful information such as drop velocities, liquid fluxes, drop number density, and SMD for spray analysis was obtained for several low injection pressure conditions. Our present processor for the phase doppler analyzer has an upper doppler frequency limit which restricts the measurements to sprays with lower speed flows. For future work, the phase doppler will be modified to use optical frequency shifting such that the doppler frequency of the scattered light signals are optically downshifted within the operating range of the processor. By applying frequency shifting to our present processor, drop velocity up to 300 m/sec can be measured. A two color phase doppler system is also under consideration for making two-component velocity measurements simultaneously. With two-component velocity information, it is possible to determine drop trajectories and to evaluate the effect of drop collision in the sprays. We also intend to use the control of detector voltage, threshold, and high and low pass filtering of the processor for closer examination of the larger drops. Using the concept of a spectrometer with a narrow band width, we can progressively tune in to sections of the size distribution spectrum and obtain more information about certain size ranges with less interference by not processing particles outside the size range of interest. In this way, we can make a more meaningful comparative study between the photographic and phase doppler results.

REFERENCES

1. Bachalo, W.D. and Houser, M.J., "Phase Doppler Spray Analyzer for Simultaneous Measurements of Drop Size and Velocity Distributions," Optical Engineering, Vol. 23, No. 5, pp. 583-590, 1984.

2. Nukiyama, S. and Tanasawa, Y., "Experiments on the Atomization of Liquids in an Airstream", Trans. Soc. Mech. Eng. Japan, Vol. 5, pp. 68-75, 1939.

3. Brazier,P.R. et. al, "The Interaction of Falling Water Drops: Coalescence," Proc. R. Soc. Lond., A. 326, pp. 393-408, 1972.

4. Podvysotsky, A.M. and Shraiber, A.A., "Coalescence and Break-Up of Drops in Two-Phase Flows", Int. J. Multiphase Flow, Vol. 10, No. 2, pp. 195-209, 1984.

5. Ahlers, K.D. and Alexander, D.R., "A Microcomputer-Based Digital Image Processing System Developed to Count and Size Laser-Generated Small Particle Images," Optical Engineering, In Press, 1985.

6. Tacina, B., NASA Lewis Research Center, Private Communication, 1985.

7. Simmons, H.C., "The Prediction of Sauter Mean Diameter for Gas Turbine Fuel Nozzles of Different Types," ASME Paper no. 79-WA/GT-5, 1979.

TABLE 1

A Summary of Phase/Doppler Results for Water Injection 45.3 lbm/hr and Air Injection 19.4 lbm/hr

	Left Hand Side						Right Hand Side				
Radial Position r(cm)	2.5	2	1.5	1	0.5	0	0.5	1	1.5	2	2.5
Mean Velocity (m/sec)	1.36	4.4	8.9	15.4	28.7	41.2	39.8	20.9	10.9	6.8	3.9
Velocity Fluctuation (m/sec)	0.85	2.5	4.6	5.9	7.5	4.6	6.4	7.4	5.3	3.2	2.1
Liq. Vol. Flux (cc/sec)	7.6×10^{-8}	5.9×10^{-7}	3.3×10^{-6}	9.0×10^{-6}	1.8×10^{-5}	1.8×10^{-4}	8.2×10^{-5}	7.9×10^{-6}	2.6×10^{-6}	1.3×10^{-6}	3.0×10^{-7}
Number Density (#/cc)	79	117	120	164	77	58	67	128	216	232	112
Temporal SMD (μm)	28	34	46	49	62	131	92	50	34	30	28

Water/Air Mass Flowrate Ratio: 2.34, x = 17 cm
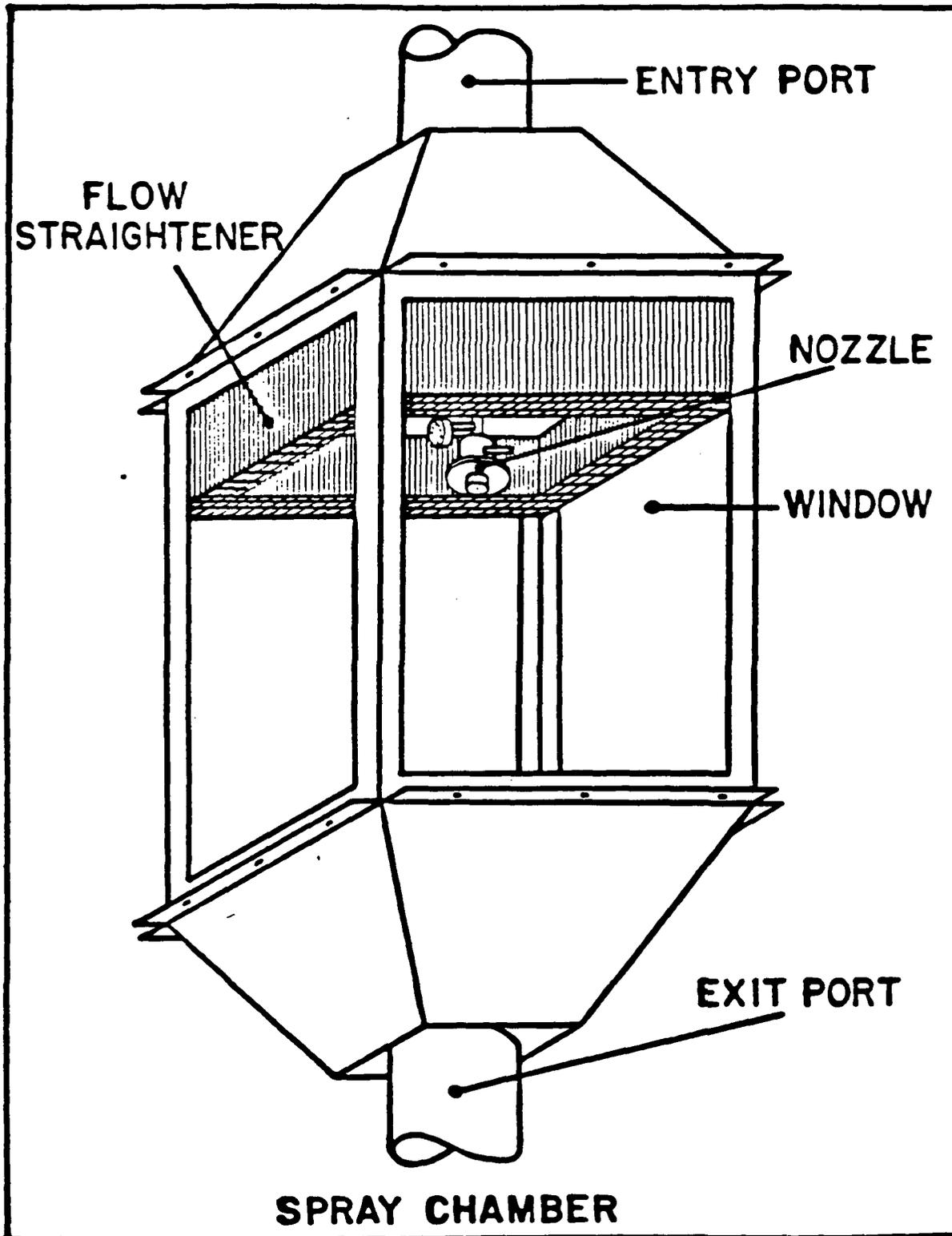
Figure 1   Schematic of the small scale spray chamber.

Secondary Air
Intake Shroud
and Flow
Straighteners

Nozzle

Viewing
Windows

4"x5" View
Camera

Sheet
Metal

Floor Level

Air Exhaust
to Blower

Catch
Tank
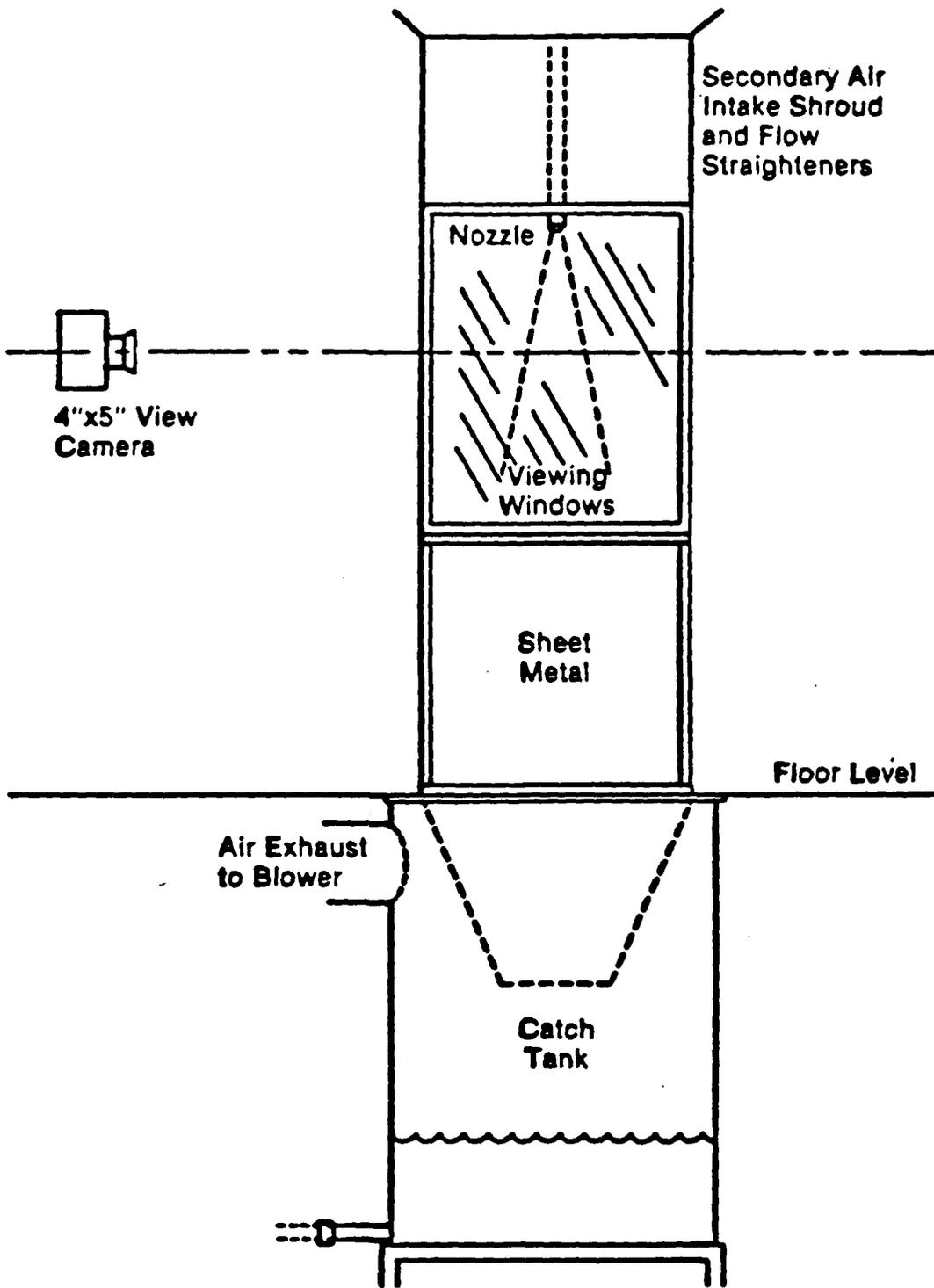
Figure 2   Schematic of the large scale spray chamber.
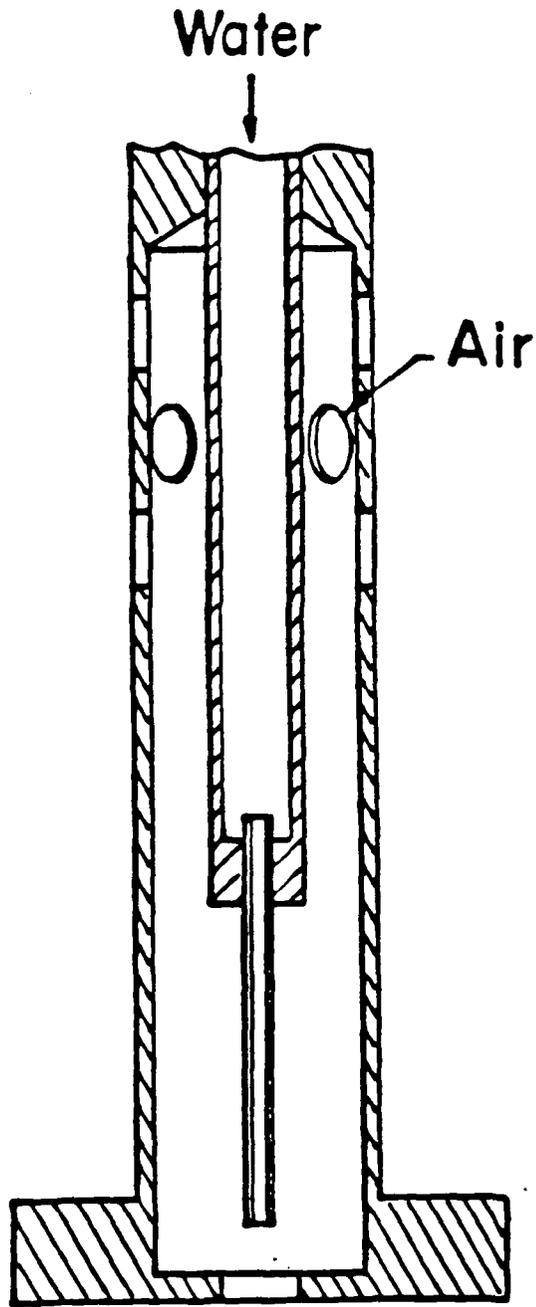
Figure 3   Cross-sectional view of NASA air-assist atomizer.
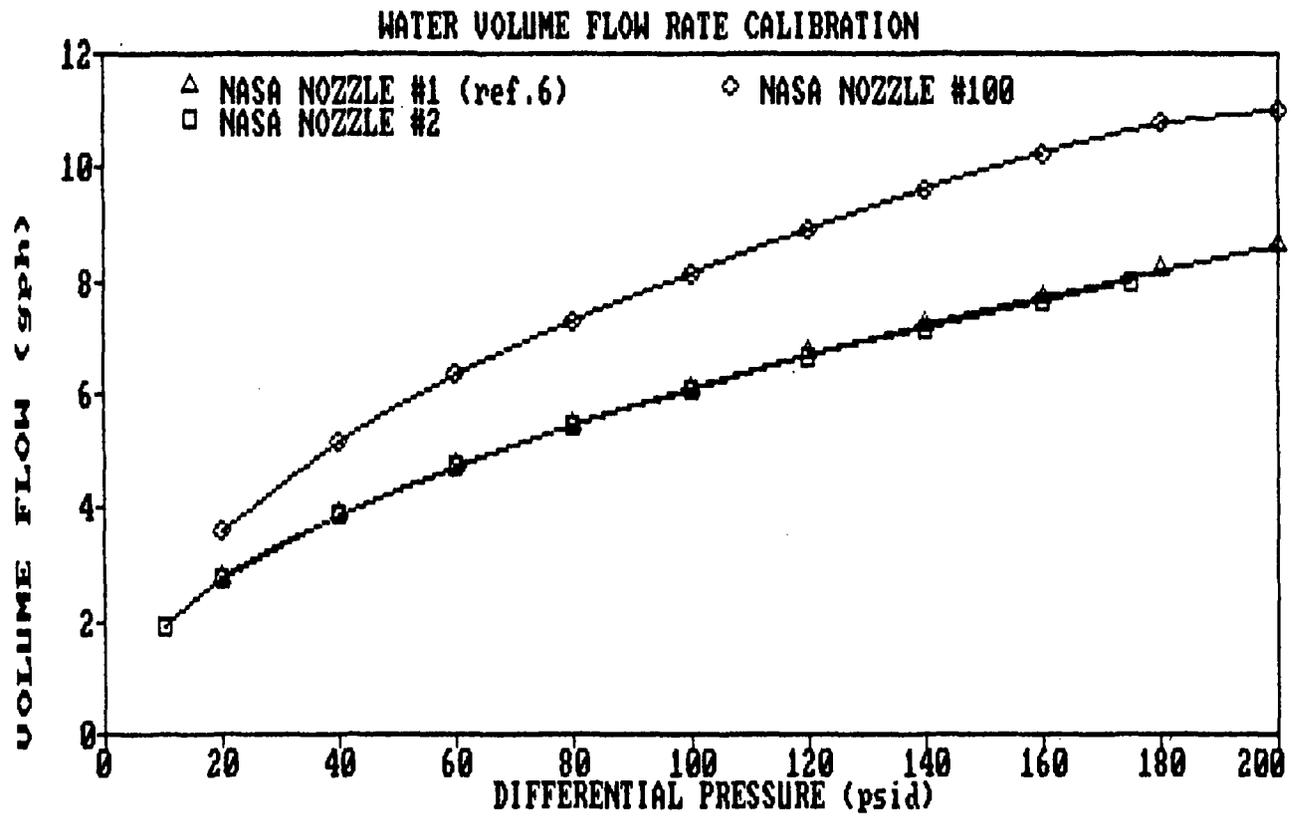
Figure 4   Water volume flow rates versus pressure difference between water and air $(P_w - P_a)$ at atomizer exit.

AIR MASS FLOW RATE CALIBRATION CURVE

△ NO WATER INJECTION

■ WITH WATER INJECTION
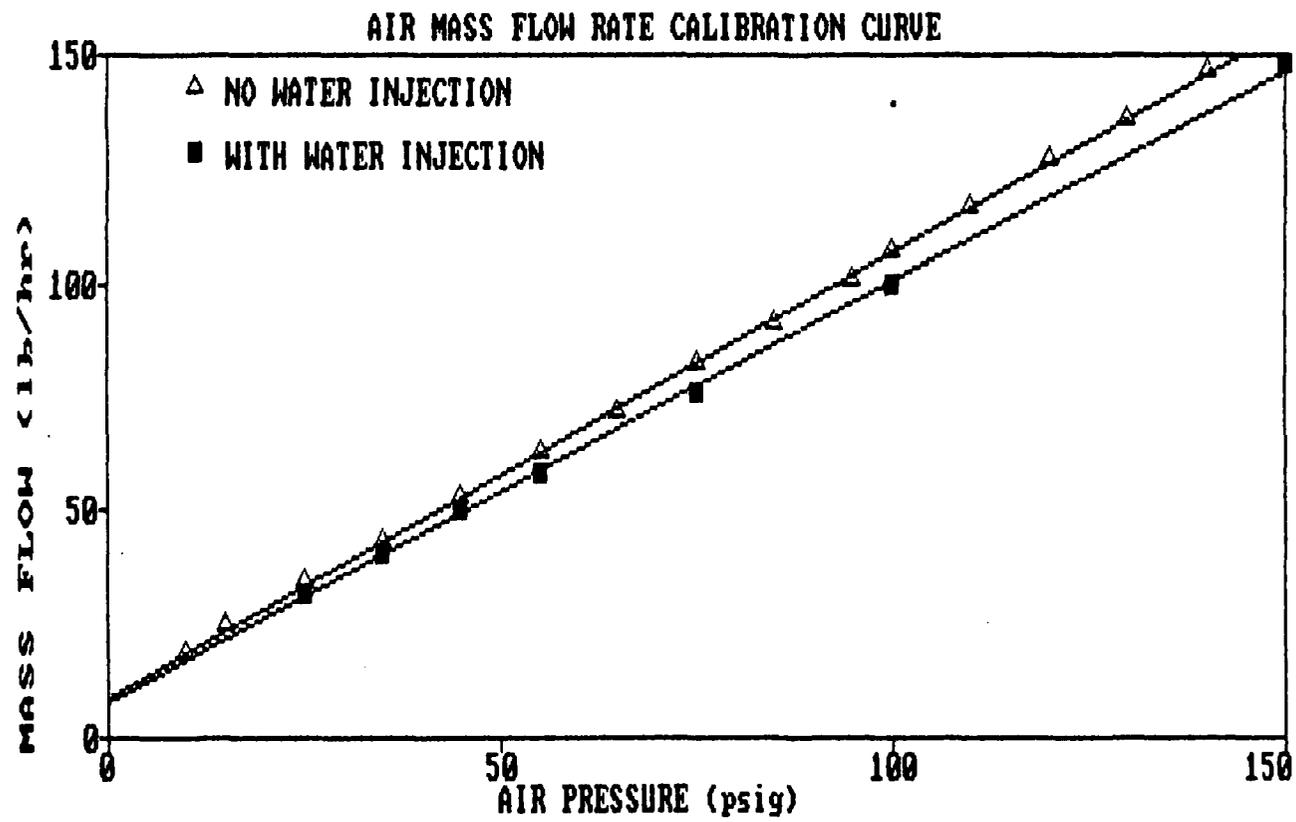
Figure 5   Air mass flow rates versus air injection pressure for nozzle #100.

AIR MASS FLOW RATE CALIBRATION CURVE

△ NO WATER INJECTION

AIR FLOW RATE (lb/hr)

AIR PRESSURE (psig)
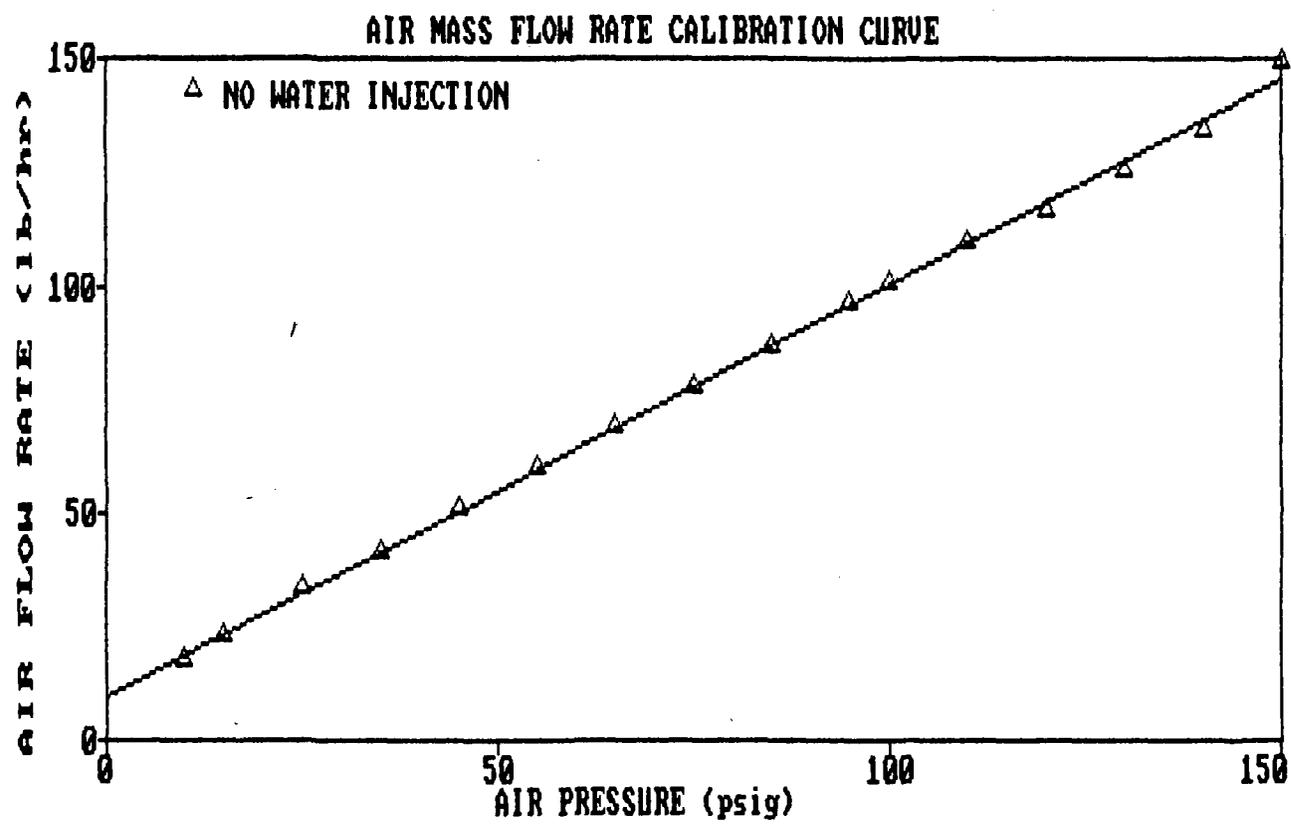
Figure 6   Air mass flow rate versus air injection pressure for nozzle #2.
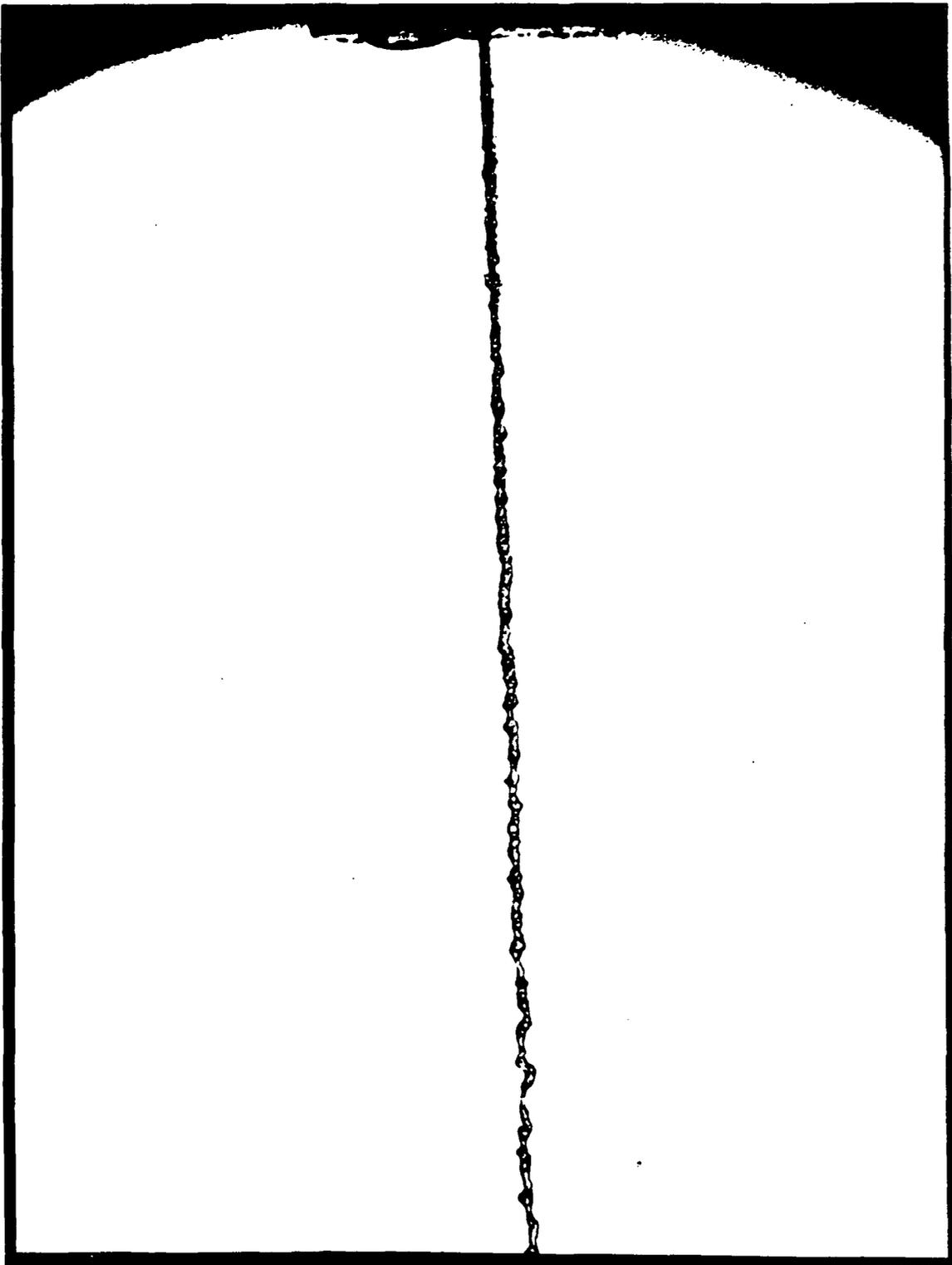
Pwater=126 psi, No Air

Figure 7
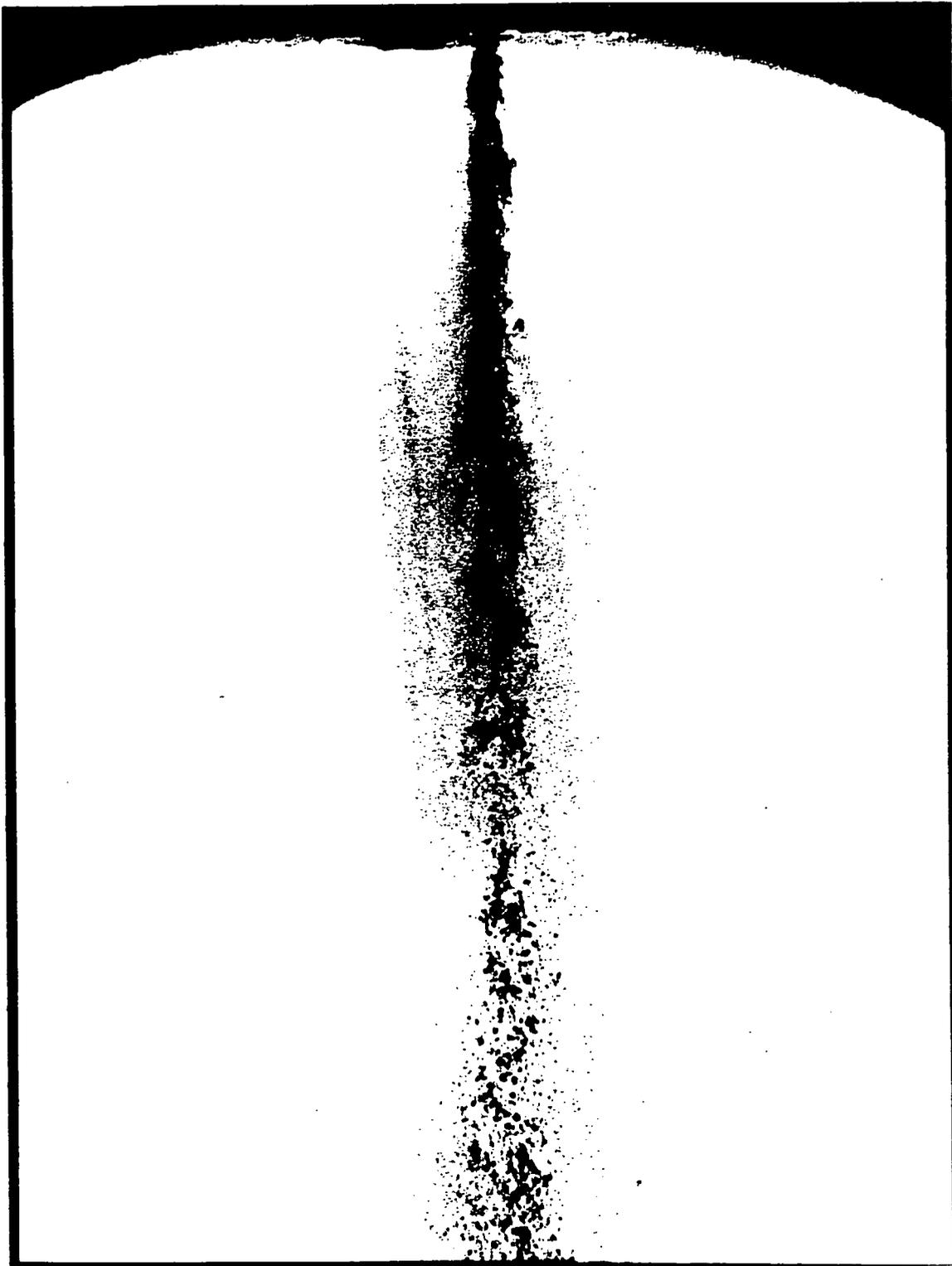
Pwater=126 psi, Pair=9.4 psi

Figure 8
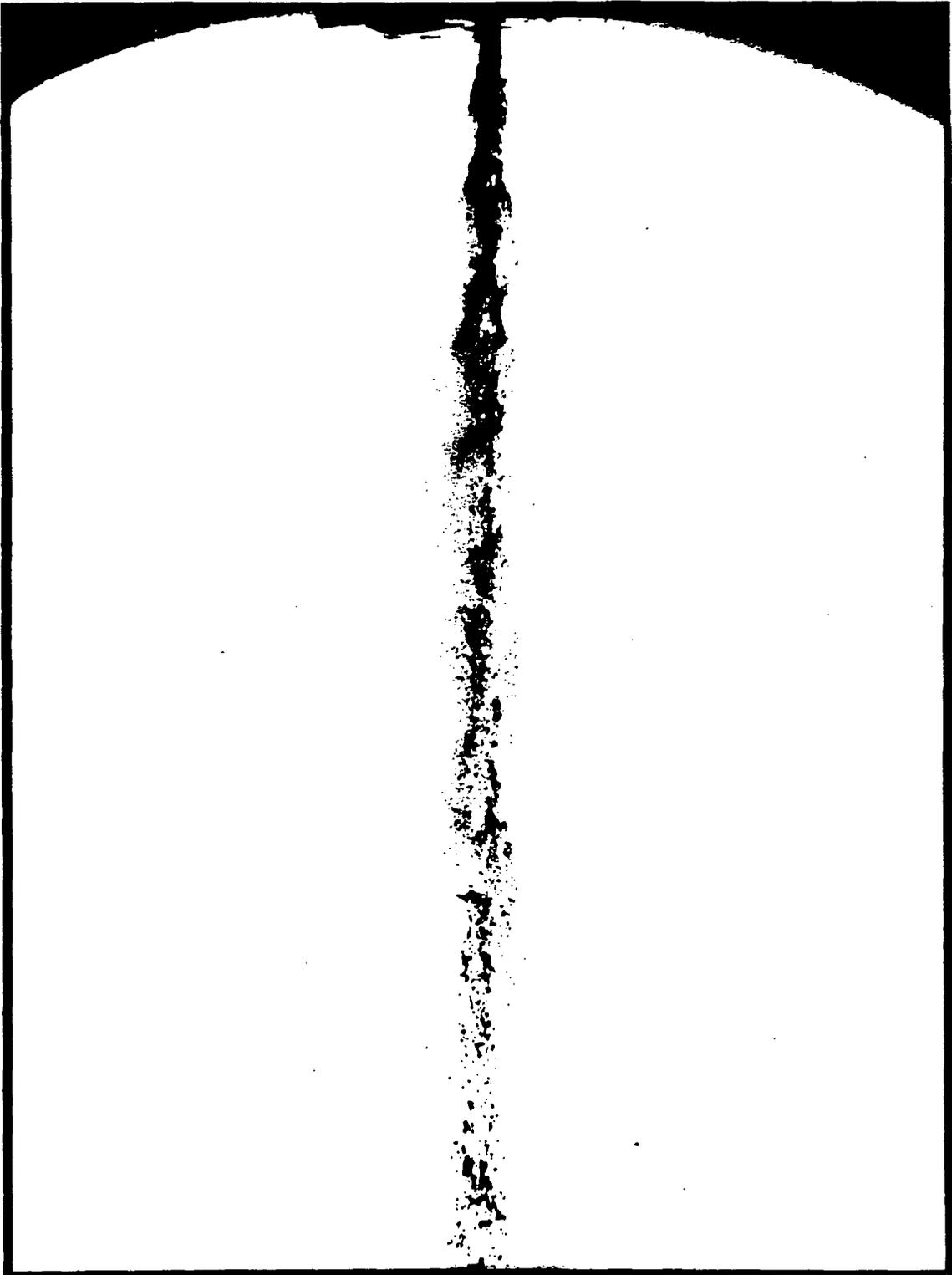
Pwater=126 psi, Pair=16.0 psi

Figure 9

Pwater=126 psi, Pair=26.6 psi

Figure 10
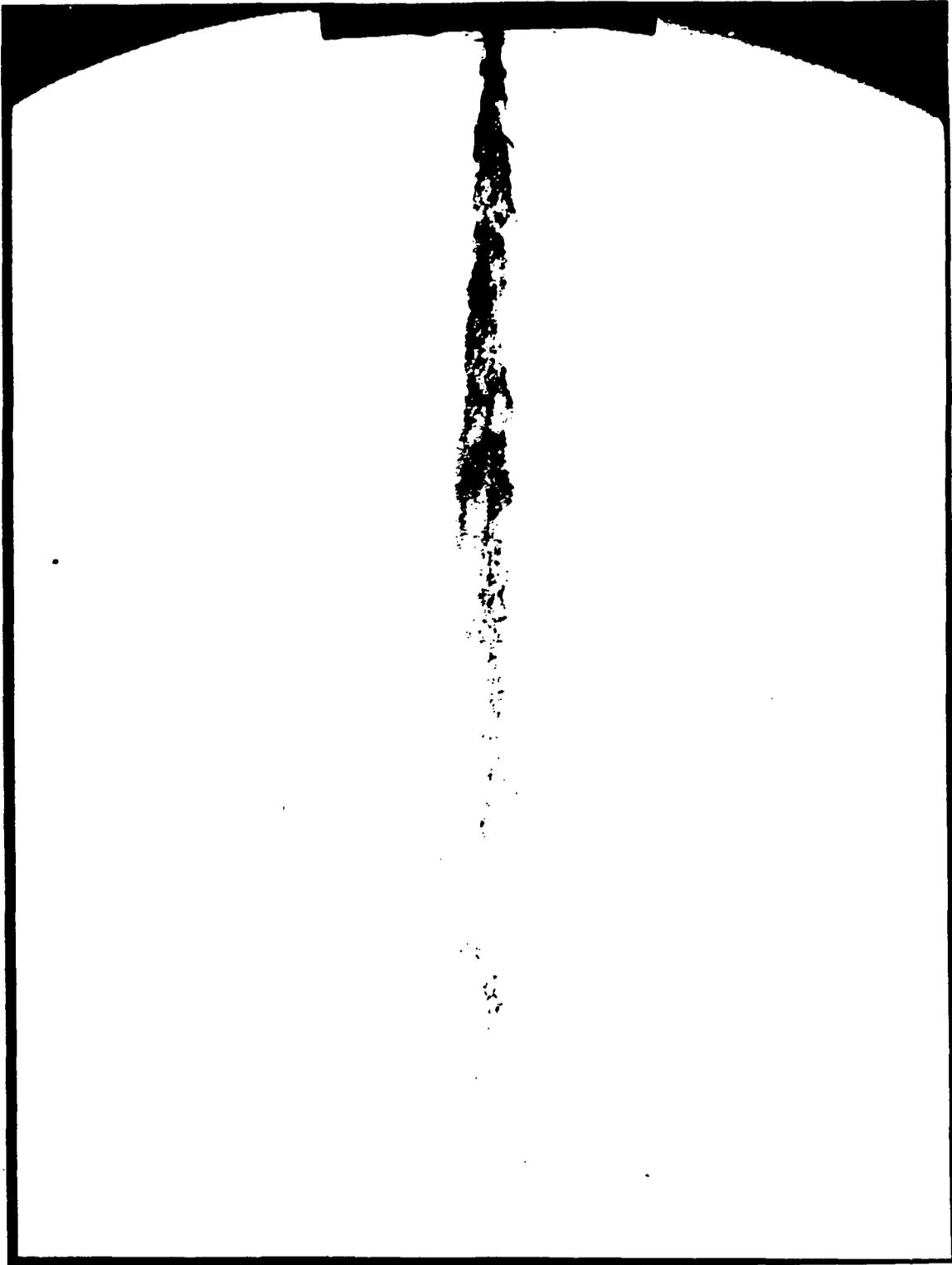
Pwater=126 psi, Pair=36.0 psi

Figure 11
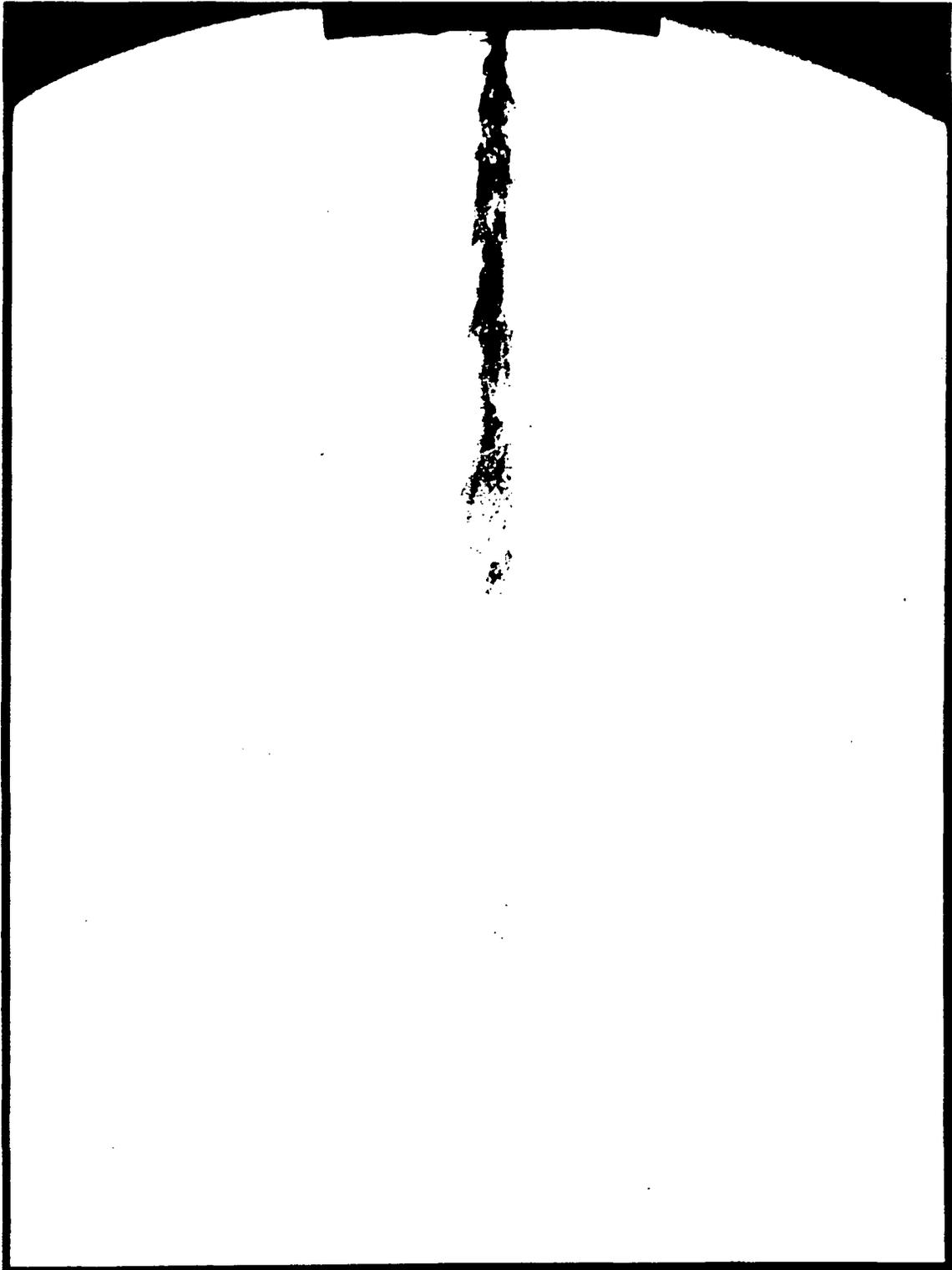
Pwater=126 psi, Pair=46.5 psi

Figure 12
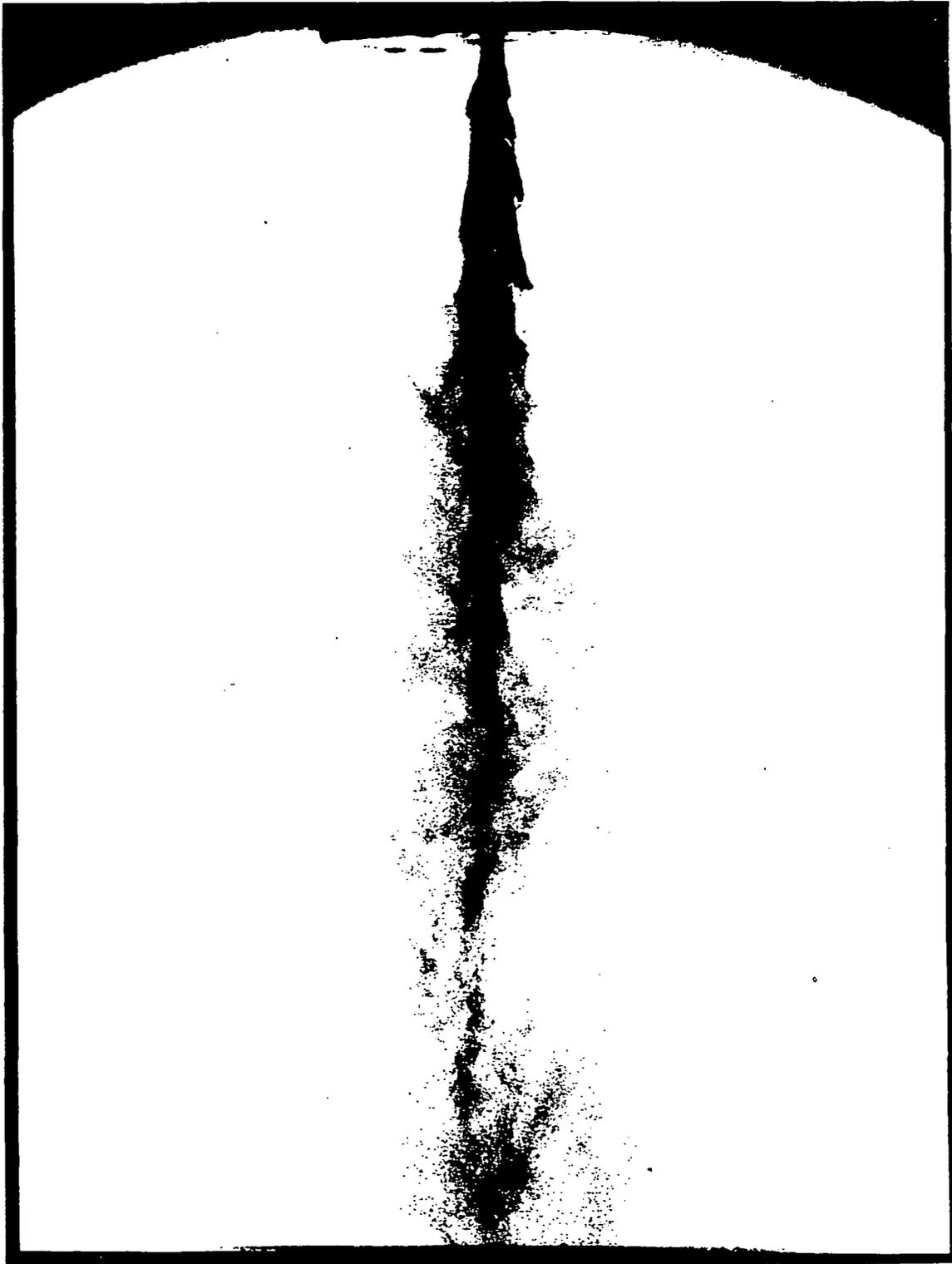
Pwater=126 psi, Pair=56.5 psi

Figure 13
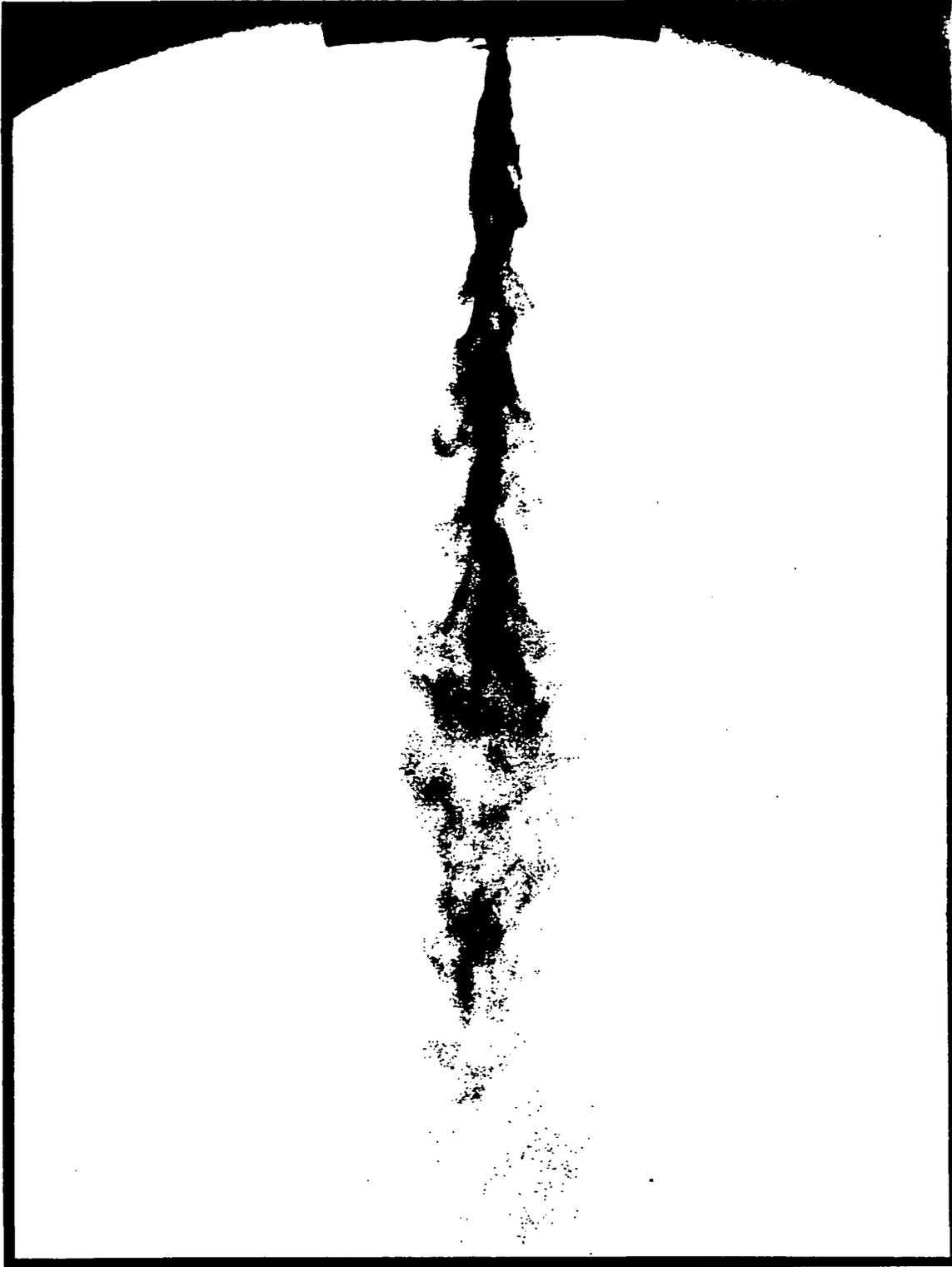
Pwater=126 psi, Pair=67.8 psi

Figure 14
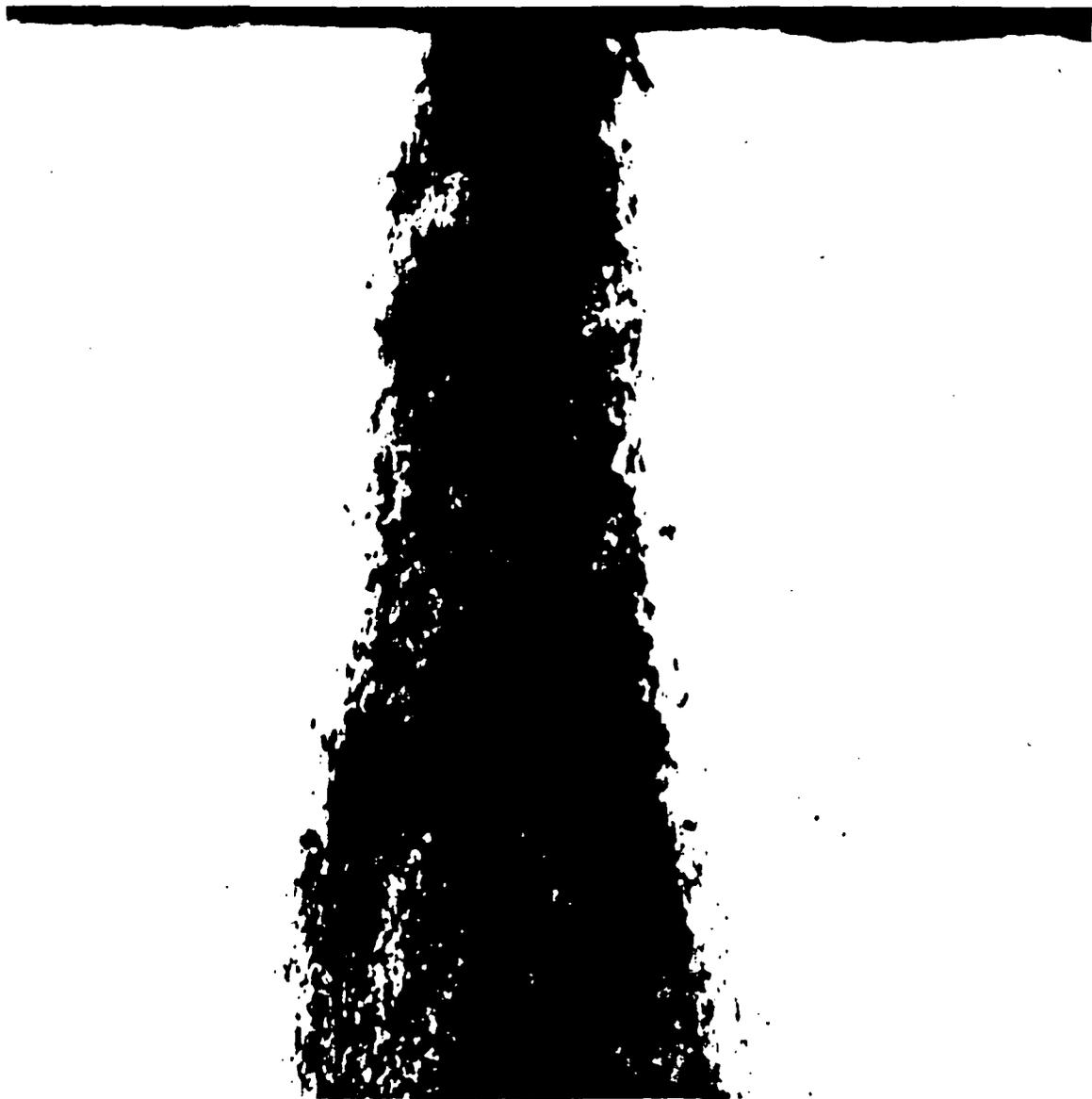
Pwater=58.7 psi, Pair=10 psi

X=0.9 cm

Figure 15

Pwater=58.7 psi, Pair=10 psi

X=2.7 cm

Figure 16

Pwater=58.7 psi, Pair=10 psi

X=4.5 cm

Figure 17

Pwater=58.7 psi, Pair=10 psi

X=6.3 cm

Figure 18

Pwater=58.7 psi, Pair=10 psi

X=8.0 cm

Figure 19
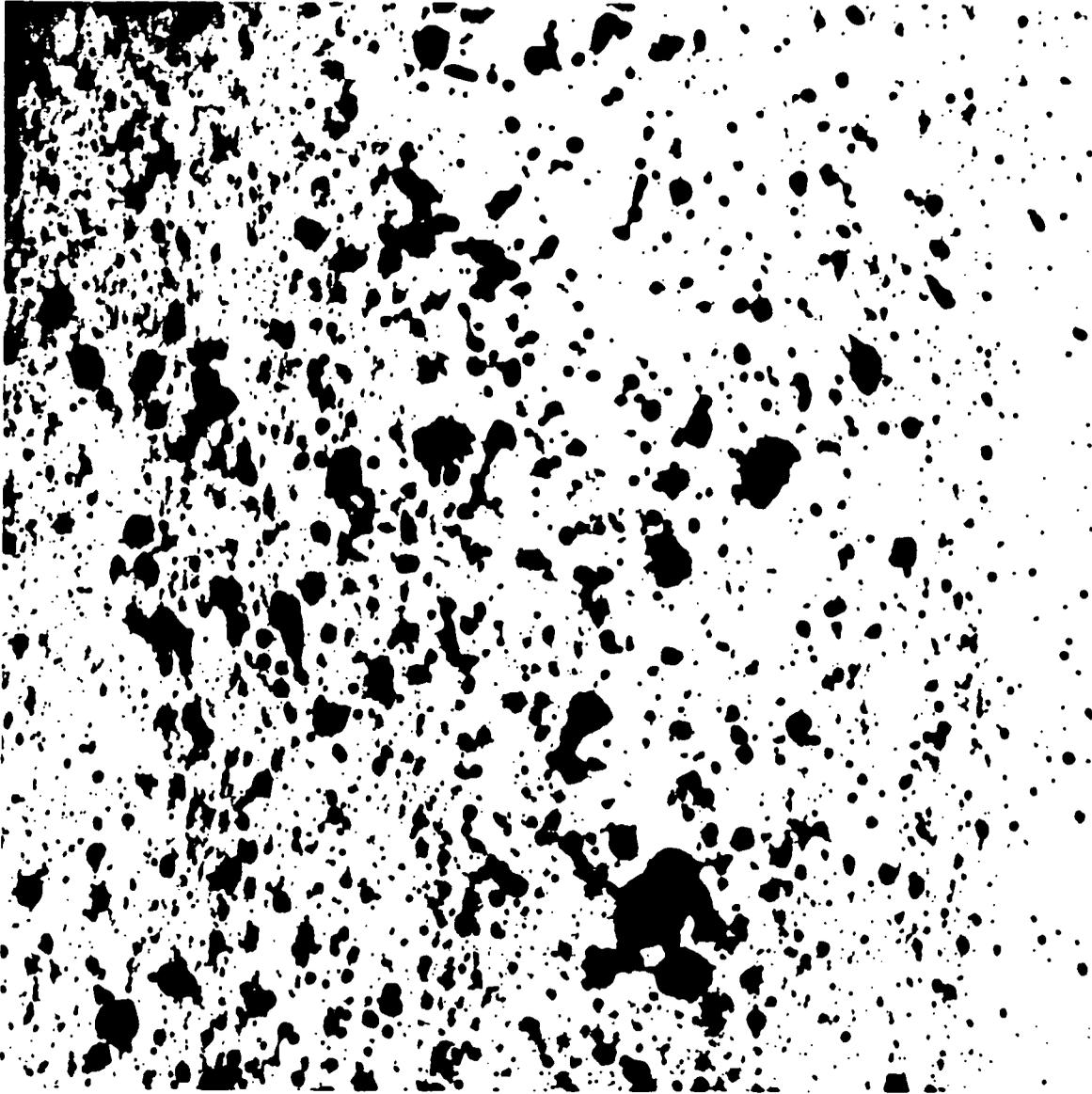
Pwater=58.7 psi, Pair=10 psi

X=10.0 cm

Figure 20

Pwater=58.7 psi, Pair=10 psi

X=11.7 cm

Figure 21
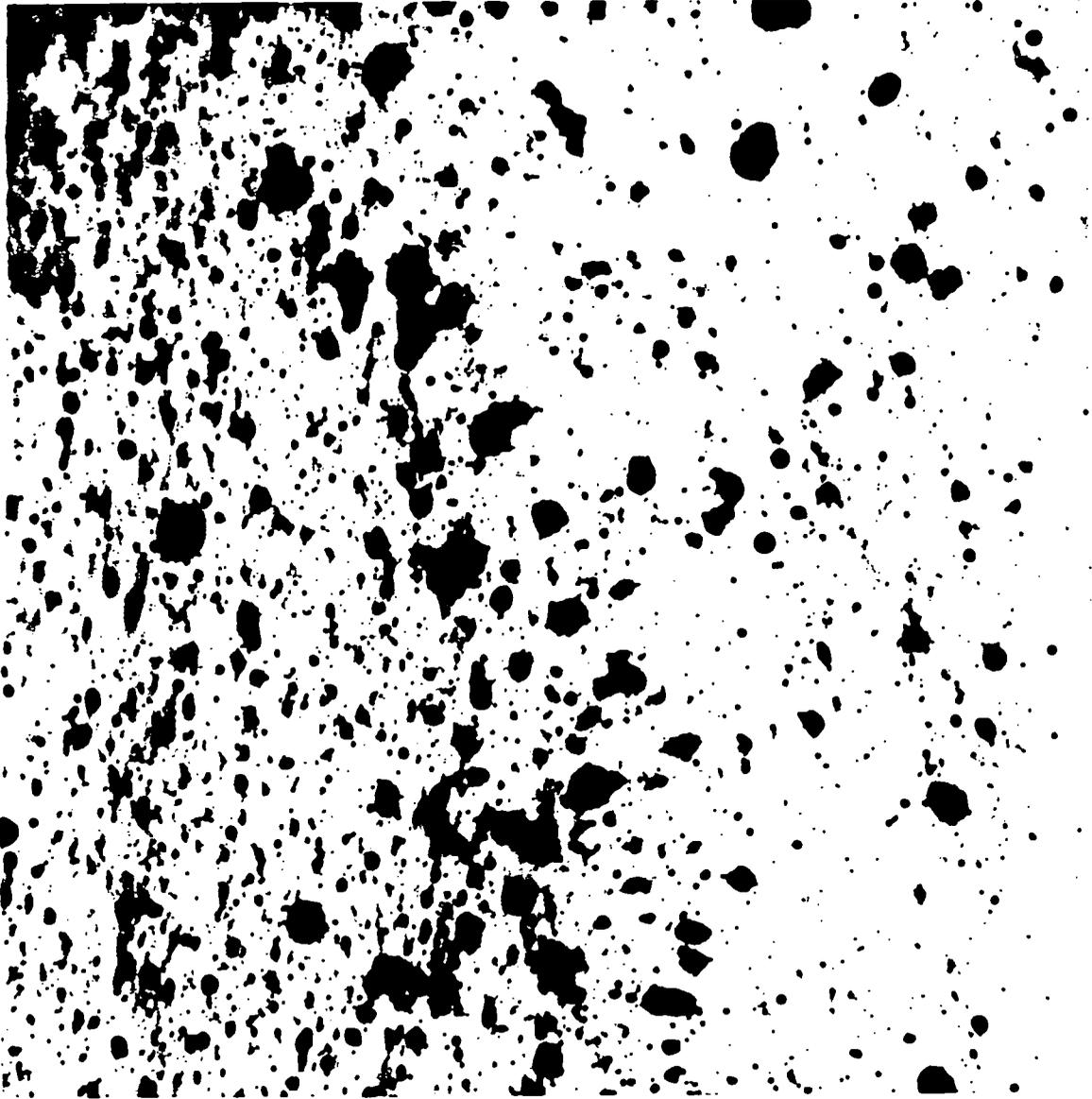
Pwater=58.7 psi, Pair=10 psi

X=13.5 cm

Figure 22
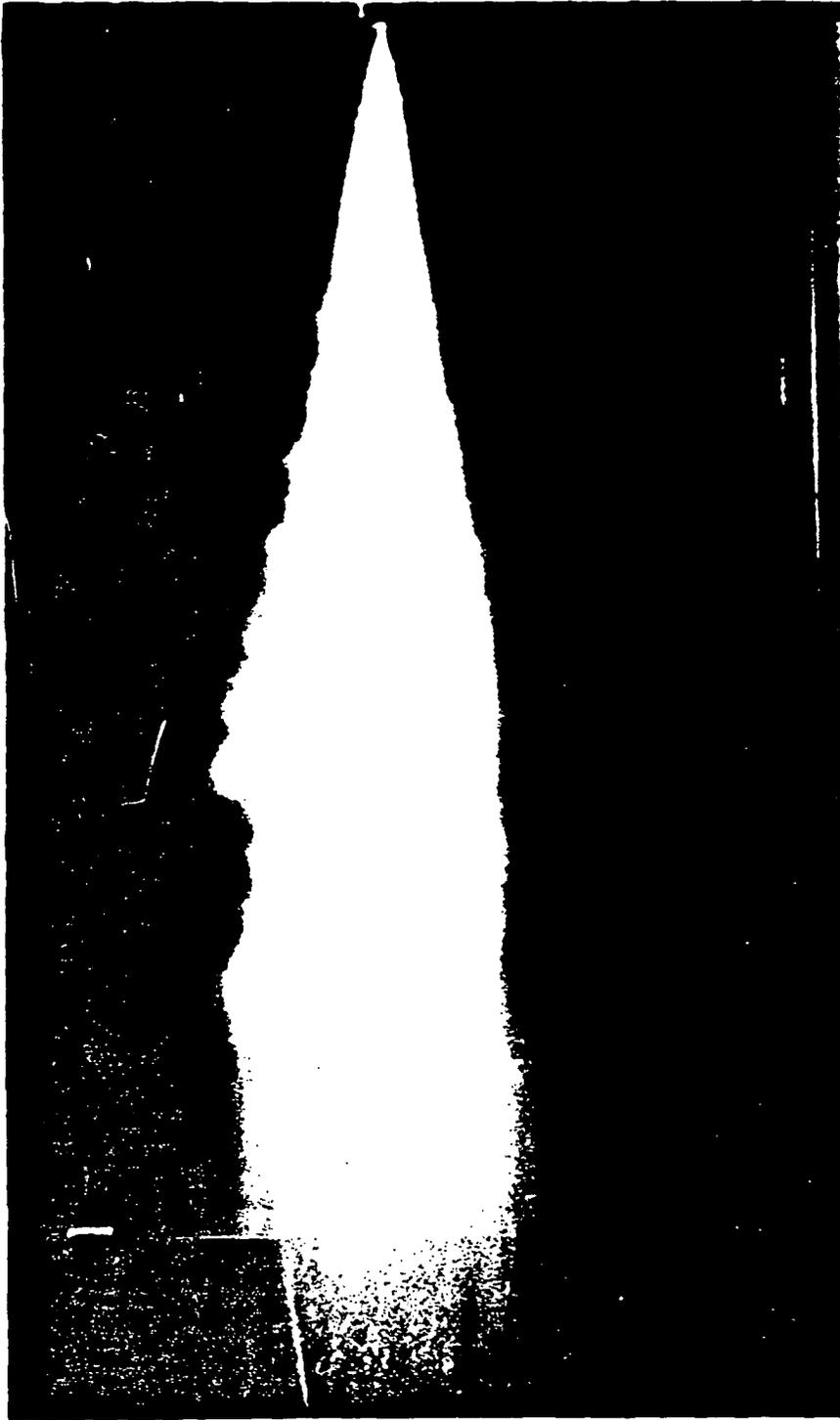
Figure 23   Spray photograph obtained by using near forward lighting technique
for the determination of spray cone angle.

SMD RADIAL DISTRIBUTION
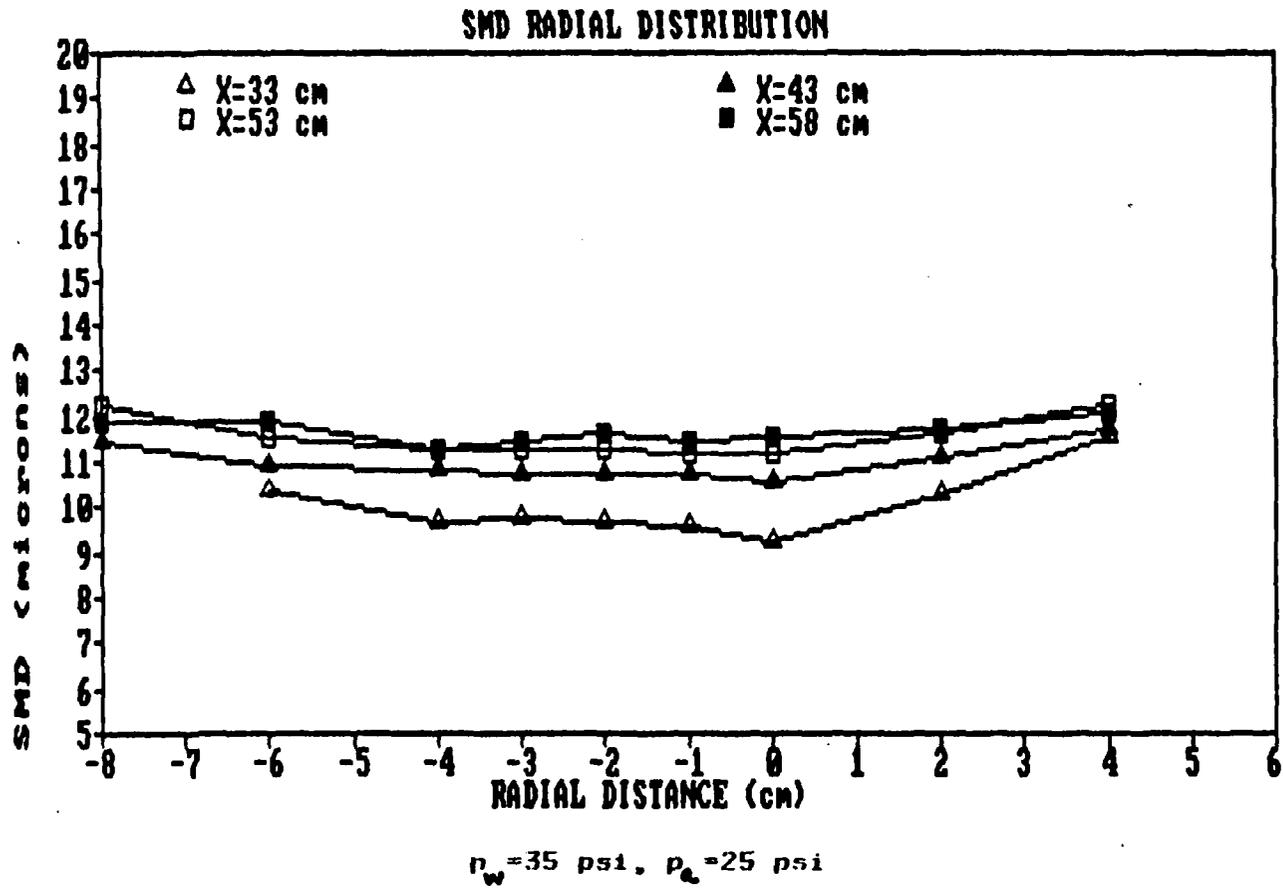
Figure 24   Radial SMD distribution at various downstream stations at P_w= 35 psi and P_{air}= 25 psi for nozzle #100.
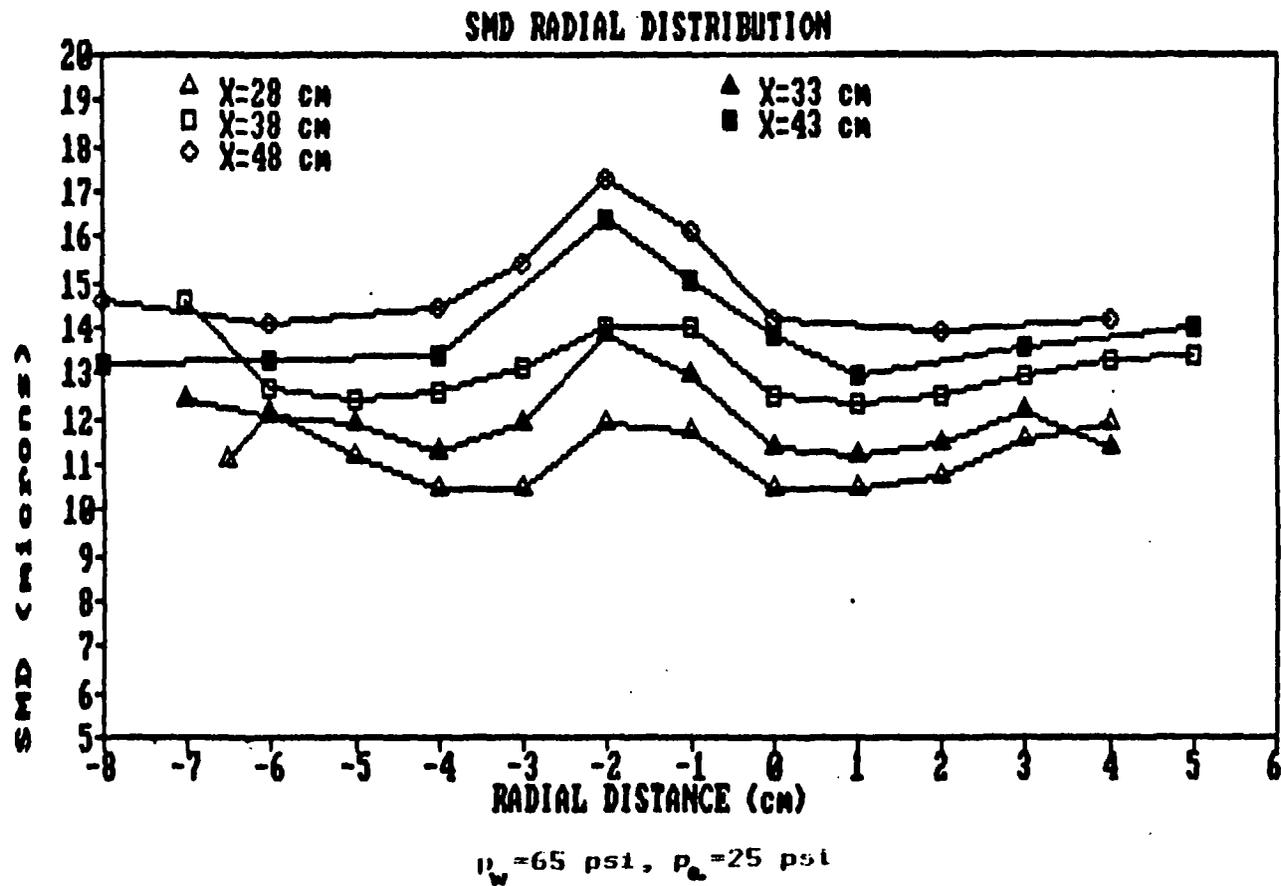
Figure 25   Radial SMD distribution at various downstream stations at P_w= 65 psi and P_{air}= 25 psi for nozzle #100.
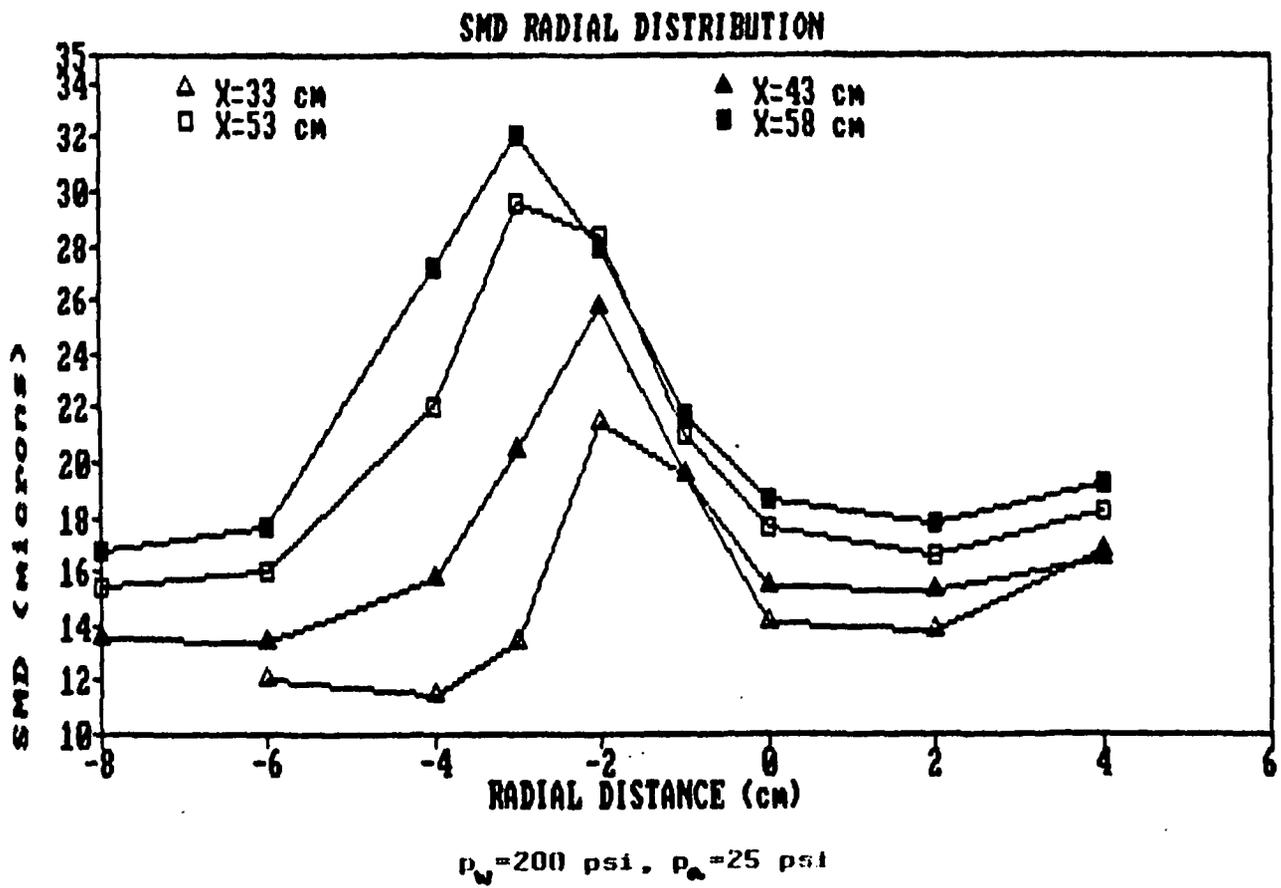
Figure 26   Radial SMD distribution at various downstream stations at P_w = 200 psi and P_{air} = 25 psi for nozzle #100.

SMD RADIAL DISTRIBUTION

△ X=33 cm   ▲ X=43 cm
□ X=53 cm   ■ X=58 cm

SMD (microns) vs RADIAL DISTANCE (cm)

P_w=200 psi, P_a=75 psi
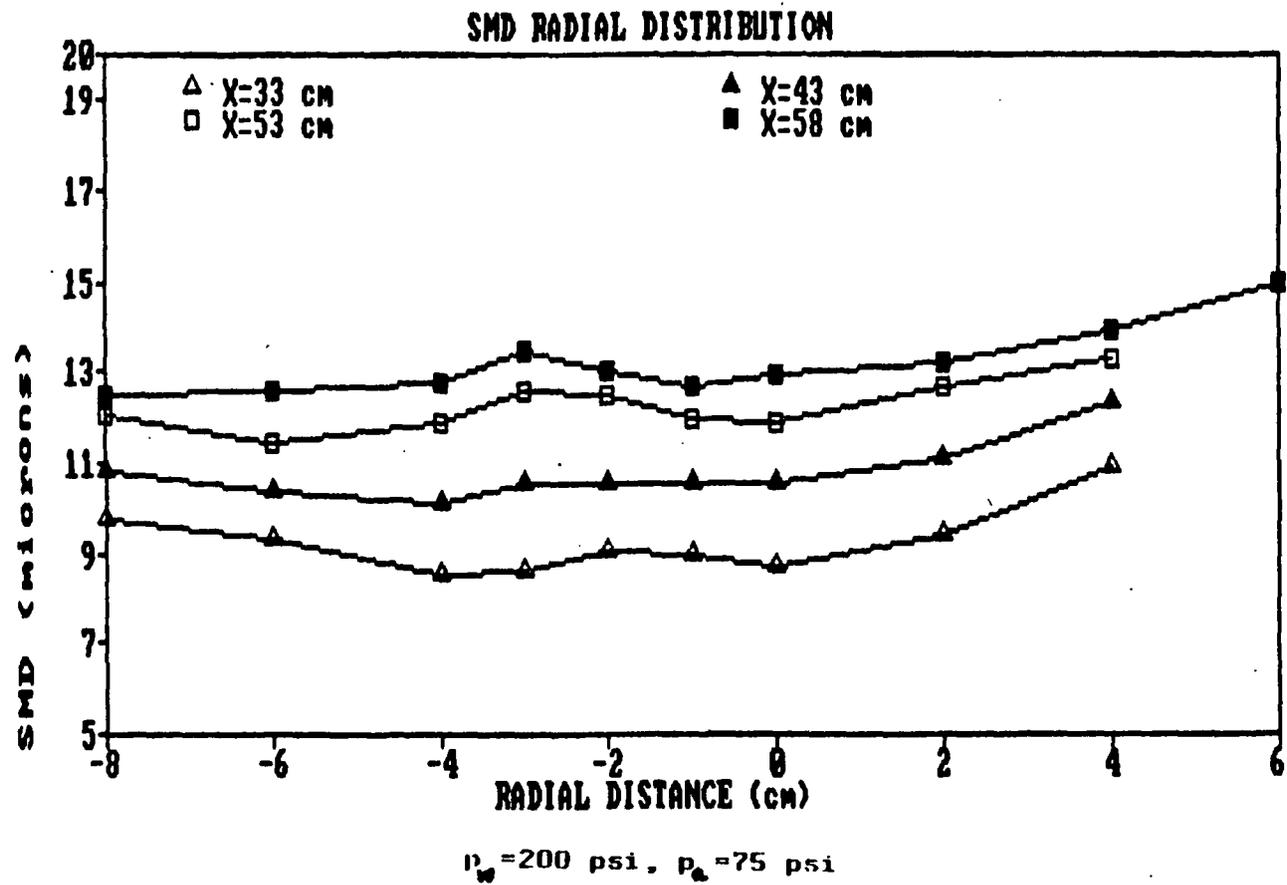
Figure 27   Radial SMD distribution at various downstream stations at P_w= 200 psi and P_{air}= 75psi for nozzle #100.
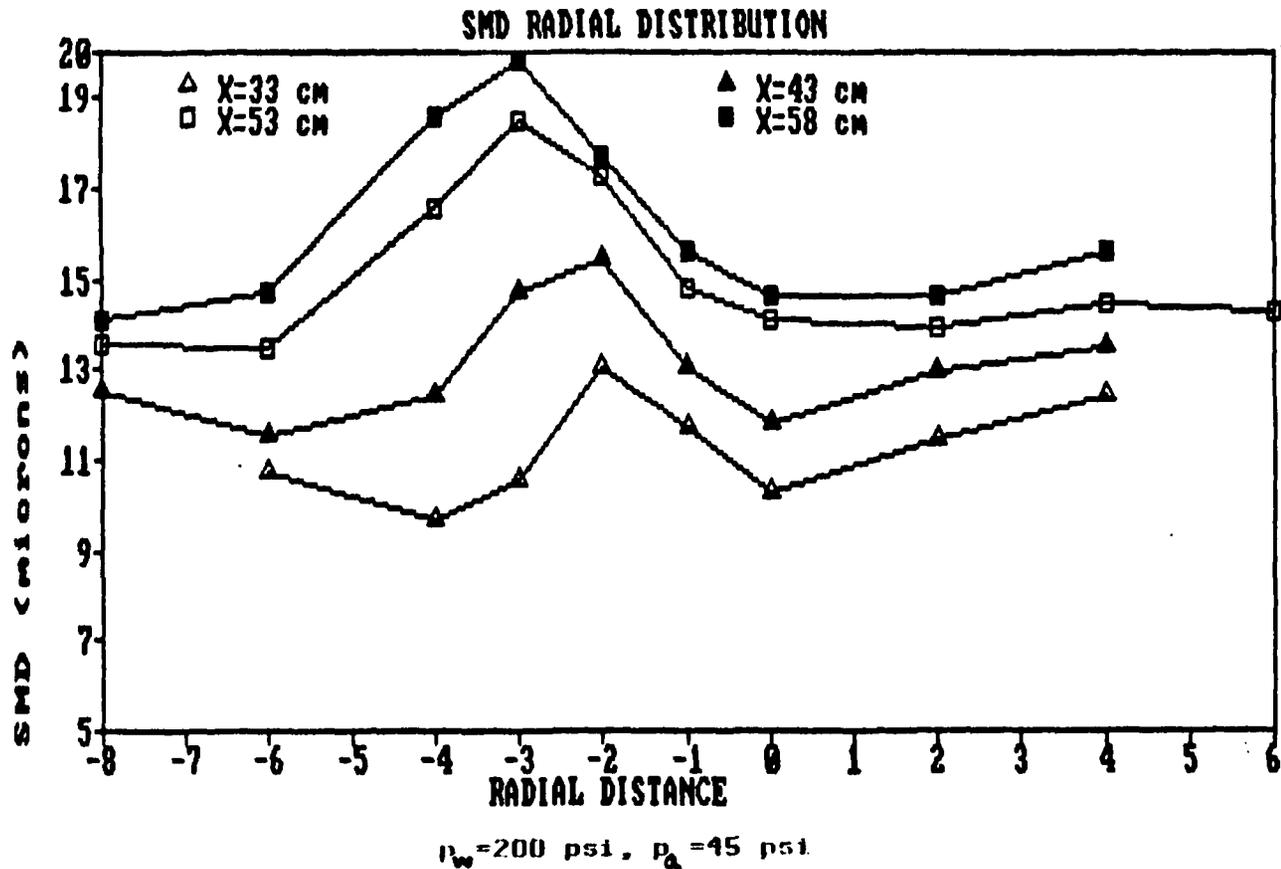
Figure 28   Radial SMD distribution at various downstream stations at P_w = 200 psi and P_{air} = 45 psi for nozzle #100.
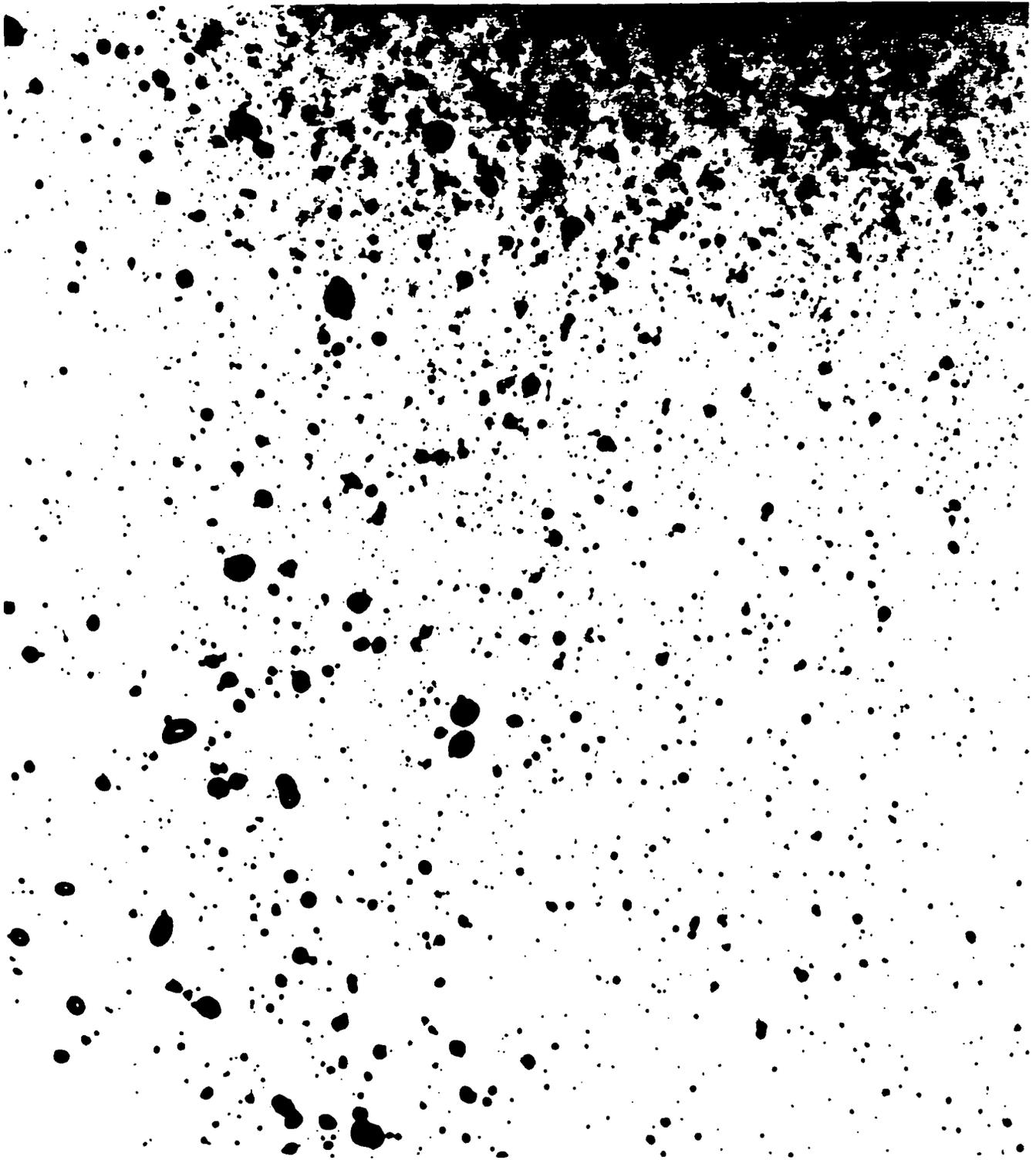
Figure 29   Picture taken at 15 cm downstream from atomizer
             with 59 psi water injection and 10 psi air
             injection.
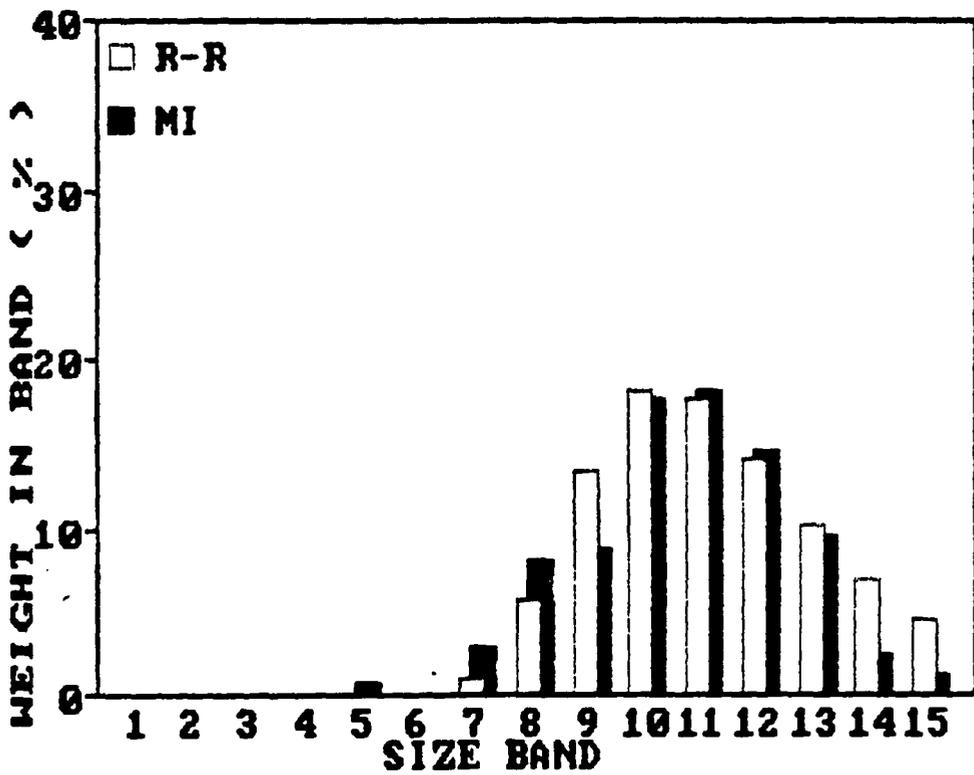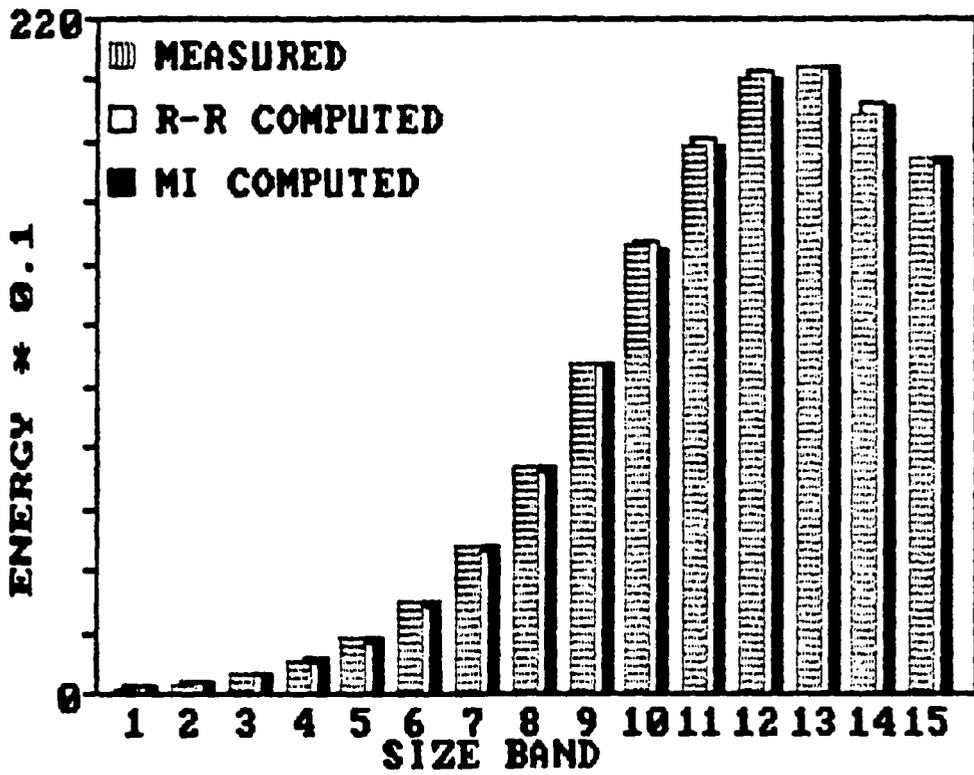
Figure 30   An example of a "good Fit" in predicting size
   distribution using the Rosin-Rammler mode.
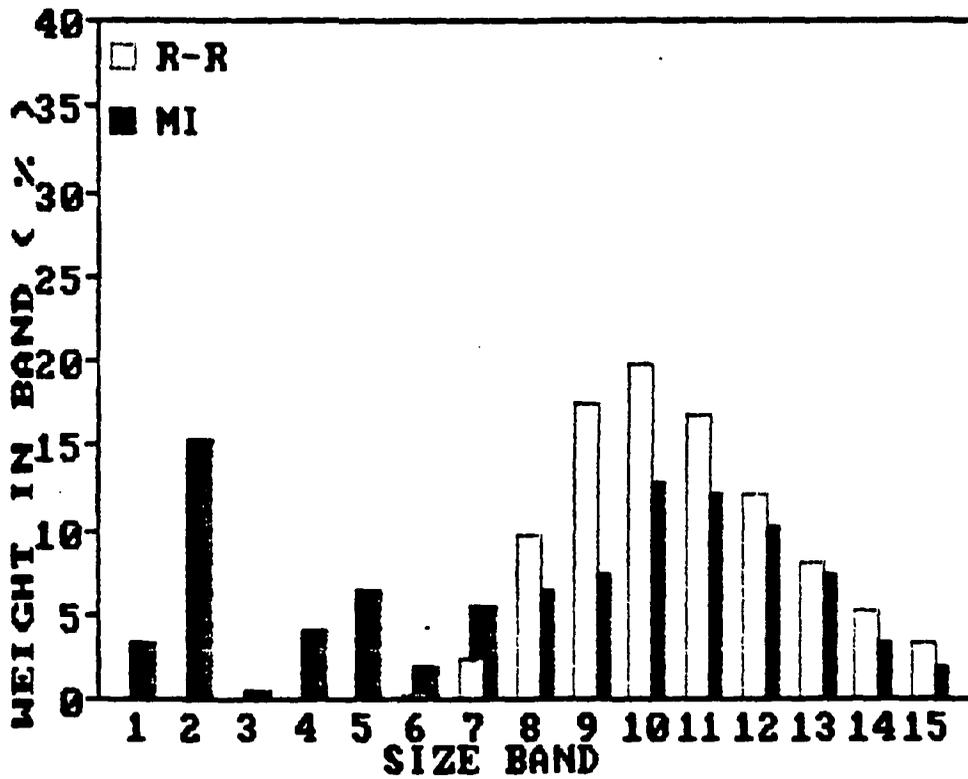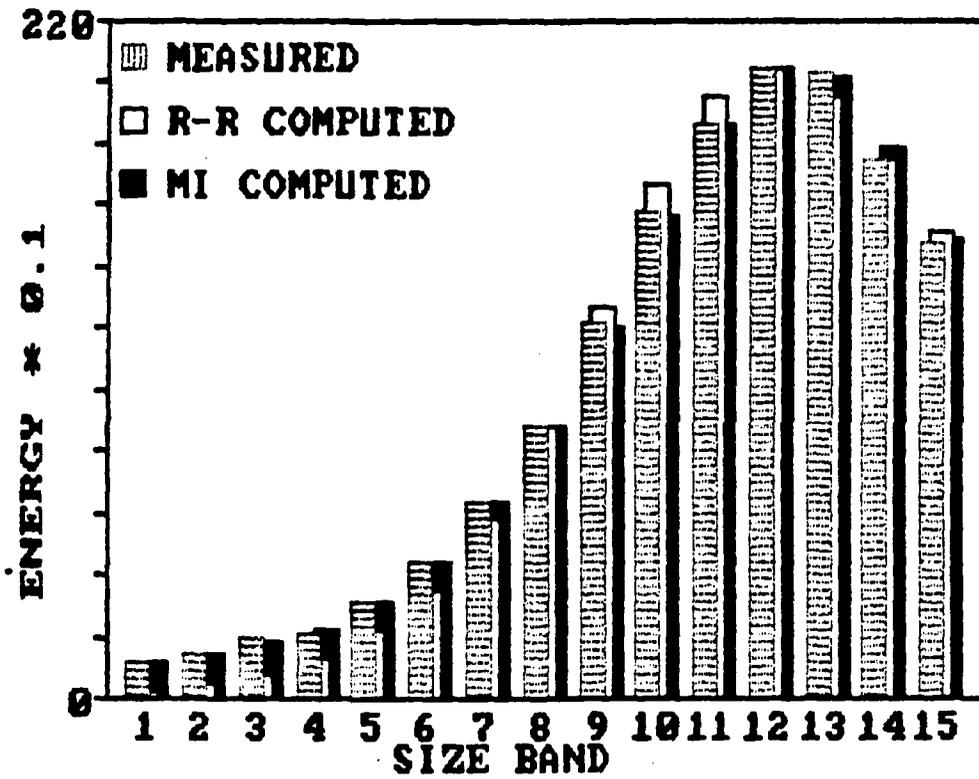
Figure 31   At the edge of the sprays the Rosin-Rammler
   mode fails to predict large size drops.

SMD RADIAL DISTRIBUTION
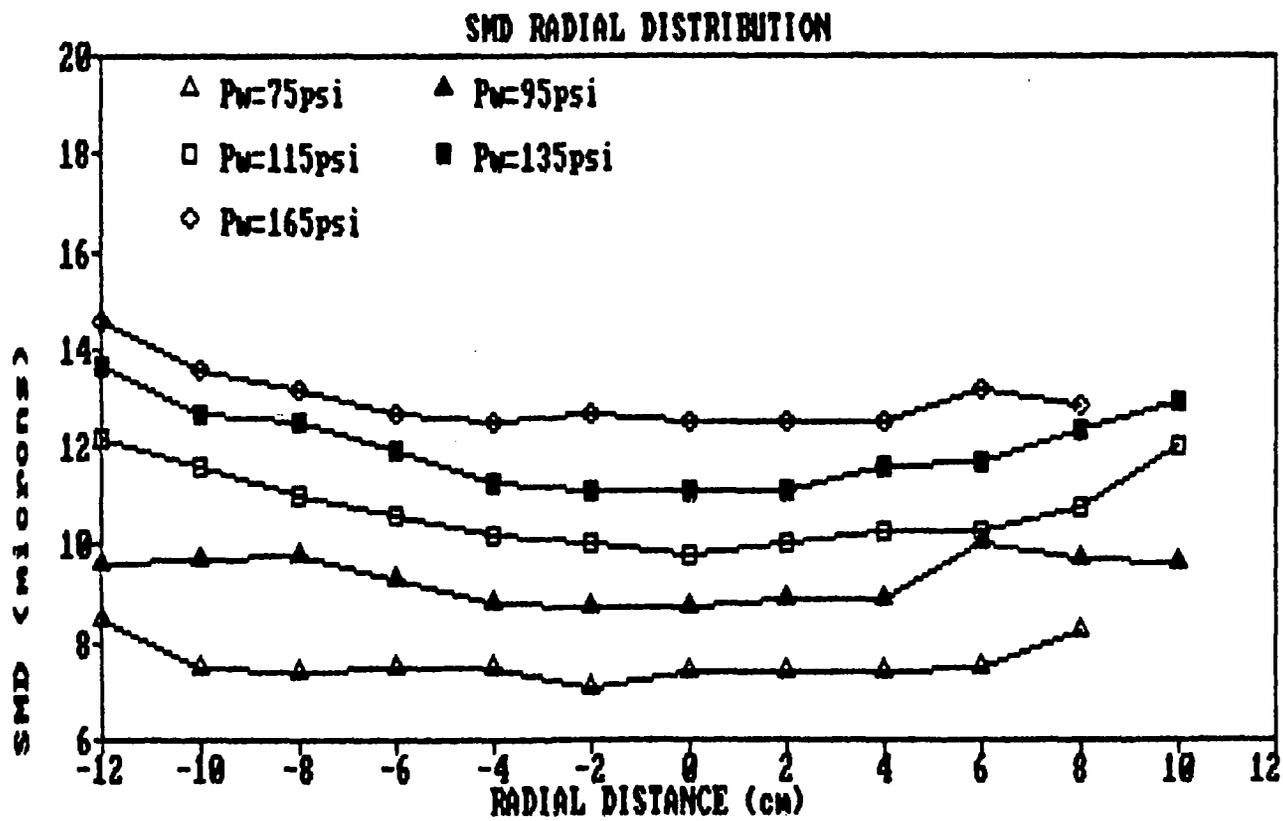
Figure 32   Radial SMD distribution at various differential pressures for nozzle #100 at P_{air}= 65 psi and downstream location x=25 inches.
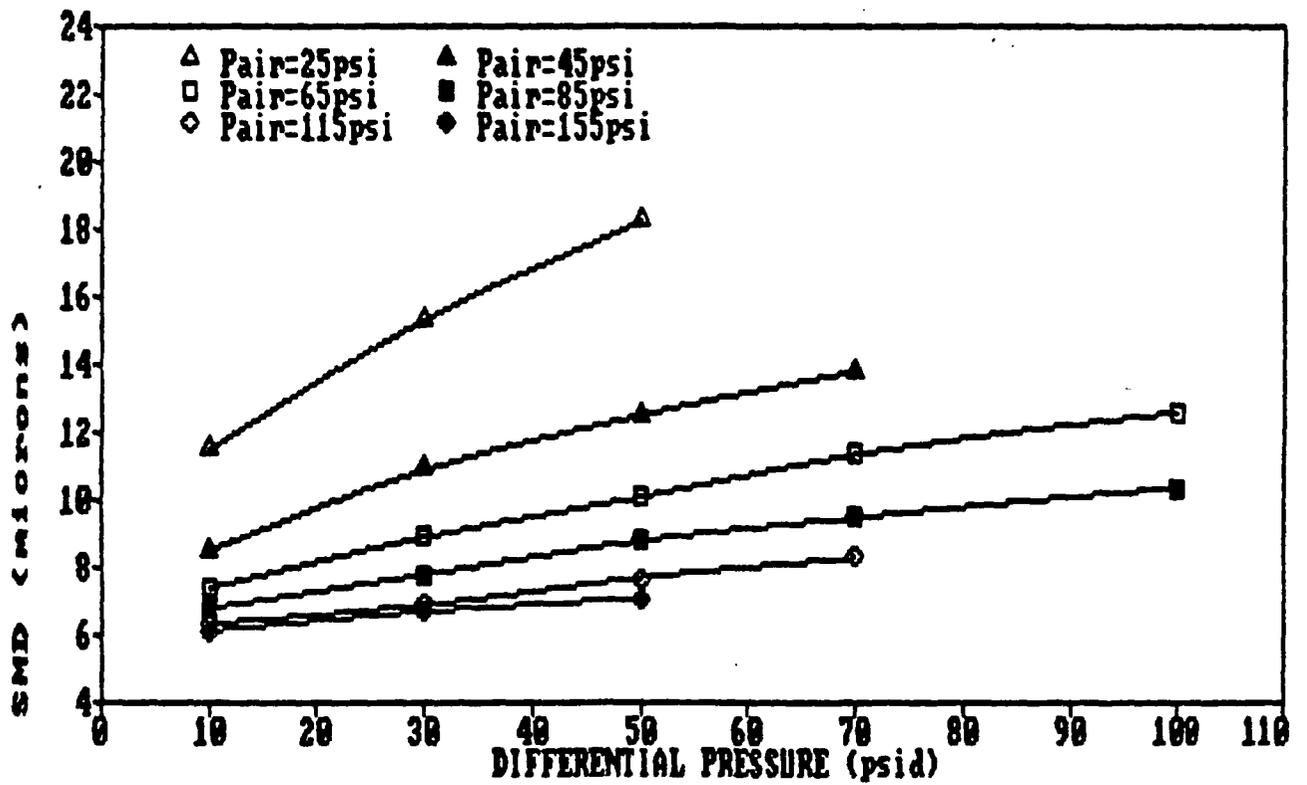
Figure 33   The variation of plane averaged SMD versus
differential pressures (P_w- P_{air}) for NASA #2
air-assist nozzle.

CORRELATION RESULTS FOR NASA #2 NOZZLE USING SF7

SMD (microns) vs.

$$\rho_A^{-.325} \left(\frac{\dot{m}_L}{\dot{m}_L V_L + \dot{m}_a V_a} \right)^{0.55}$$
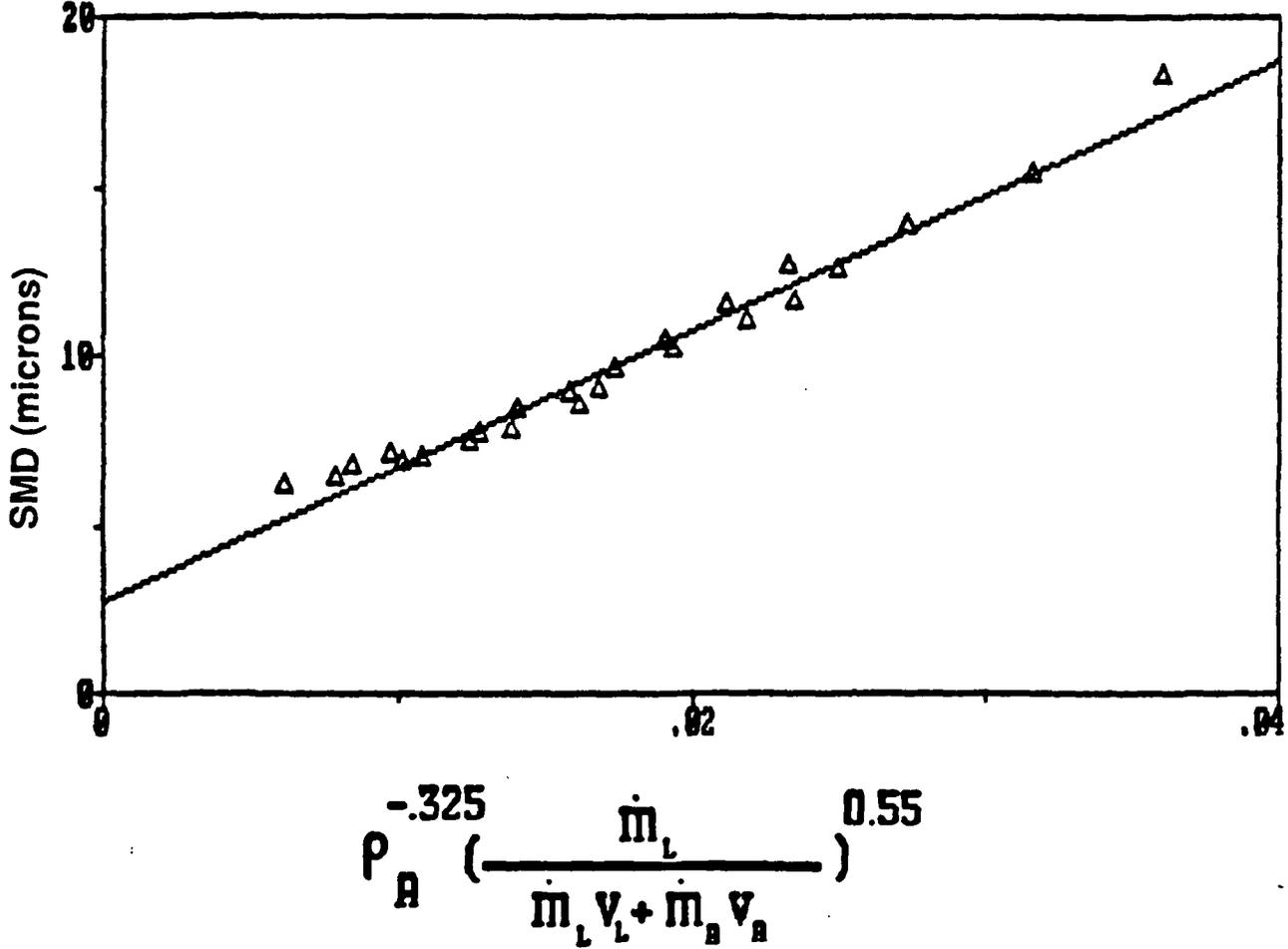
Figure 34   SMD correlation for NASA #2 nozzle using Simmons' equation.